promoter, and it has been shown that C/EBPβ-FL and LIP respectively, function as positive and negative regulators of C/EBPα gene expression [44]. Thus it is probable that LIP preferentially binds to the C/EBP-binding elements not only on the albumin promoter but also on that of C/EBPα at the expense of C/EBPβ-FL, LAP and C/EBPα. However, LIP lacks the transactivation domain and is unable to activate transcription. LIP expression induced by ATRA possibly down-regulates the gene expression of albumin and C/EBPα, by competing for DNA-binding sites as a LIP homodimer and/or by antagonizing the transcriptional activity of C/EBP transactivators via heterodimer formation with C/EBP-FL or LAP [37]. Hence, an increase in the ratio of LIP to C/EBP transactivators is critical for down-regulation of the expression of albumin and C/EBPα genes that is mediated by ATRA. This conclusion is supported by transient transfection experiments which indicated that the activity of the albumin promoter is stimulated by transfection with C/EBPβ-FL or C/EBPα expression constructs (Figure 6A), whereas its activity is decreased by co-transfection with a LIP construct (Figure 6B). Decreased expression of C/EBPα may also contribute to the transcriptional repression of the albumin gene, since C/EBPα is known to be one of the positive regulators of albumin expression [32,33].

A key question is: how does ATRA differentially induce C/EBPβ-LIP but not C/EBPβ-FL expression? A previous study [45], which describes the effect of ATRA on the alternate production of C/EBPβ isoforms, has not demonstrated its molecular mechanism. A number of recent observations have shown that the production of C/EBPβ isoforms is regulated by epidermal growth factor [38], lipopolysacharide [44,46] and partial hepatectomy [44,47], presumably through leaky ribosomal scanning [34,37]. It has been proposed that a portion of ribosomes ignore the first two AUG codons of the C/EBPβ mRNA and initiate translation of LIP from the third in-frame AUG start codon. The translation of LIP can be controlled by specific cytoplasmic proteins that interact with the 5' end region of C/EBPβ mRNA, such as CUG-BP1 (CUG triplet-repeat binding protein 1) [44,47]. Phosphorylation of CUG-BP1 is critical for its RNA binding and the consequent increase in LIP expression [38]. Therefore we tested whether ATRA treatment leads to increased phosphorylation of CUG-BP1 in FLC-4 cells. Western blotting and immunoprecipitation of CUG-BP1 metabolically labelled with ^{32}P, however, indicated that the expression level and phosphorylation status of CUG-BP1 were not different in cells with or without ATRA treatment (results not shown). It can be speculated that other RNA-binding proteins are involved in the mechanism by which ATRA increases the translation of LIP because, in addition to CUG-BP1, calreticulin [48] and eIFs (eukaryotic translation initiation factors), such as eIF-2 and eIF-4E [35], have been shown to control translation of C/EBPβ. Another possible mechanism for the alternate production of C/EBPβ isoforms is the proteolytic cleavage of C/EBPβ-FL [49]. However, this is less likely to explain the mechanism for the differential induction of LIP isoforms caused by ATRA, because it has been shown that the cleavage of C/EBPβ-FL to generate LIP is induced by C/EBPα [49], but that the ATRA treatment led to no change or only a small decrease in the expression of C/EBPα (Figure 5A).

A previous study [13] has shown that the expression of HNF-1, which is a potent transcription factor for the albumin gene [50], was decreased in human hepatoma cells in which albumin gene expression was down-regulated by ATRA, although an upstream regulatory region of the albumin gene involved in the regulation was not identified. In our experimental setting, mRNA expression of HNF-1 was not affected by ATRA treatment (Figures 3A and

3B). The data in the present study suggest a model in which the preferential increase in LIP expression mediated by ATRA results in the antagonization of C/EBP transactivators by interaction with their binding sites on the nt -367 to -167 region of the albumin promoter. We propose a novel pathway for the modulation of gene expression by ATRA, in which C/EBPβ-LIP plays a crucial role. This mechanism may be found in other systems for physiological processes, such as cell proliferation and differentiation, and the elucidation of its molecular mechanism will make a great contribution to our understanding of gene regulation mediated by retinoic acids.

REFERENCES

1   West, J. B. (1990) Blood and the plasma proteins: functions and composition of blood. In Physiological Basis of Medical Practice. In (West, J. B., ed.), pp. 332–338, Williams & Wilkins, Baltimore

2   Rothschild, M. A., Oratz, M. and Schreiber, S. S. (1988) Serum albumin. Hepatology 8, 385–401

3   Moshage, H. J., Janssen, J. A., Franssen, J. H., Hafkenscheid, J. C. and Yap, S. H. (1987) Study of the molecular mechanism of decreased liver synthesis of albumin in inflammation. J. Clin. Invest. 79, 1635–1641

4   Mariani, G., Strober, W., Keiser, H. and Waldmann, T. A. (1976) Pathophysiology of hypoalbuminemia associated with carcinoid tumor. Cancer 38, 854–860

5   Chlebowski, R. T., Grosvenor, M. B., Bernhard, N. H., Morales, L. S. and Bulcavage, L. M. (1989) Nutritional status, gastrointestinal dysfunction, and survival in patients with AIDS. Am. J. Gastroenterol. 84, 1288–1293

6   Phillips, A., Shaper, A. G. and Whincup, P. H. (1989) Association between serum albumin and mortality from cardiovascular disease, cancer, and other causes. Lancet 2, 1434–1436

7   Gorski, K., Carneiro, M. and Schibler, U. (1986) Tissue-specific in vitro transcription from the mouse albumin promoter. Cell 47, 767–776

8   Maire, P., Wuarin, J. and Schibler, U. (1989) The role of cis-acting promoter elements in tissue-specific albumin gene expression. Science 244, 343–346

9   Perlmutter, D. H., Dinarello, C. A., Punsal, P. I. and Colten, H. R. (1986) Cachectin/tumor necrosis factor regulates hepatic acute-phase gene expression. J. Clin. Invest. 78, 1349–1354

10 Andus, T., Geiger, T., Hirano, T., Kishimoto, T. and Heinrich, P. C. (1988) Action of recombinant human interleukin 6, interleukin 1β and tumor necrosis factor α on the mRNA induction of acute-phase proteins. Eur. J. Immunol. 18, 739–746

11 Morrone, G., Cortese, R. and Sorrentino, V. (1989) Post-transcriptional control of negative acute phase genes by transforming growth factor β. EMBO J. 8, 3767–3771

12 Hsu, S. L., Lin, Y. F. and Chou, C. K. (1992) Transcriptional regulation of transferrin and albumin genes by retinoic acid in human hepatoma cell line Hep3B. Biochem. J. 283, 611–615

13 Yamada, Y., Shidoji, Y., Fukutomi, Y., Ishikawa, T., Kaneko, T., Nakagama, H., Imawari, M., Moriwaki, H. and Muto, Y. (1994) Positive and negative regulations of albumin gene expression by retinoids in human hepatoma cell lines. Mol. Carcinog. 10, 151–158

14 Molina, A., Oka, T., Muñoz, S. M., Chikamori-Aoyama, M., Kuwahata, M. and Natori, Y (1997) Vitamin B$_6$ suppresses growth and expression of albumin gene in a human hepatoma cell line HepG2. Nutr. Cancer 28, 206–211

15 Tsutsumi, T., Nakao, K., Mitsuoka, S., Hamasaki, K., Tsuruta, S., Shima, M., Nakata, K., Tamaoki, T. and Nagataki, S. (1993) Regulation of albumin and α-fetoprotein gene expression by colloid osmotic pressure in human hepatoma cells. Gastroenterology 104, 256–262

16 Pietrangelo, A. and Shafritz, D. A. (1994) Homeostatic regulation of hepatocyte nuclear transcription factor 1 expression in cultured hepatoma cells. Proc. Natl. Acad. Sci. U.S.A. 91, 182–186

17 Marten, N. W., Hsiang, C. H., Yu, L., Stollenwerk, N. S. and Straus, D. S. (1999) Functional activity of hepatocyte nuclear factor-1 is specifically decreased in amino acid-limited hepatoma cells. Biochim. Biophys. Acta 1447, 160–174

18 Falasca, L., Favale, A., Gualandi, G., Maietta, G. and Conti Devirgiliis, L. (1998) Retinoic acid treatment induces apoptosis or expression of a more differentiated phenotype on different fractions of cultured fetal rat hepatocytes. Hepatology 28, 727–737

19 Alisi, A., Leoni, S., Piacentani, A. and Conti Devirgiliis, L. (2003) Retinoic acid modulates the cell-cycle in fetal rat hepatocytes and HepG2 cells by regulating cyclin-cdk activities. Liver Int. 23, 179–186

20 Ikeda, H. and Fujiwara, K. (1993) Retinoic acid inhibits DNA and albumin synthesis stimulated by growth factor in adult rat hepatocytes in primary culture. Biochem. Biophys. Res. Commun. 191, 675–680

21 Sani, B. P. and Meeks, R. G. (1983) Subacute toxicity of all-trans- and 13-cis-isomers of N-ethyl retinamide, N-2-hydroxyethyl retinamide, and N-4-hydroxyphenyl retinamide. Toxicol. Appl. Pharmacol. 70, 228–235

22 Decensi, A., Bruno, S., Costantini, M., Torrisi, R., Curotto, A., Gatteschi, B., Nicolò, G., Polizzi, A., Perloff, M., Malone, W. F. and Bruzzi, P. (1994) Phase IIa study of fenretinide in superficial bladder cancer, using DNA flow cytometry as an intermediate end point. J. Natl. Cancer Inst. 86, 138–140

23 Kalemkerian, G. P., Slusher, R., Ramalingam, S., Gadgeel, S. and Mabry, M. (1995) Growth inhibition and induction of apoptosis by fenretinide in small-cell lung cancer cell lines. J. Natl. Cancer Inst. 87, 1674–1680

24 Maurer, B. J., Metelitsa, L. S., Seeger, R. C., Cabot, M. C. and Reynolds, C. P. (1999) Increase of ceramide and induction of mixed apoptosis/necrosis by N-(4-hydroxyphenyl)-retinamide in neuroblastoma cell lines. J. Natl. Cancer Inst. 91, 1138–1146

25 Puduvalli, V. K., Yung, W. K., Hess, K. R., Kuhn, J. G., Groves, M. D., Levin, V. A., Zwiebel, J., Chang, S. M., Cloughesy, T. F., Junck, L. et al. (2004) Phase II study of fenretinide (NSC 374551) in adults with recurrent malignant gliomas: a North American brain tumor consortium study. J. Clin. Oncol. 22, 4282–4289

26 Nagamori, S., Hasumura, S., Matsuura, T., Aizaki, H. and Kawada, M. (2000) Developments in bioartificial liver research: concepts, performance, and applications. J. Gastroenterol. 35, 493–503

27 Aizaki, H., Nagamori, S., Matsuda, M., Kawakami, H., Hashimoto, O., Ishiko, H., Kawada, M., Matsuura, T., Hasumura, S., Matsuura, Y. et al. (2003) Production and release of infectious hepatitis C virus from human liver cell cultures in the three-dimensional radial-flow bioreactor. Virology 314, 16–25

28 Niwa, H., Yamamura, K. and Miyazaki, J. (1991) Efficient selection for high-expression transfectants with a novel eukaryotic vector. Gene 108, 193–199

29 Iwahori, T., Matsuura, T., Maehashi, H., Sugo, K., Saito, M., Hosokawa, M., Chiba, K., Masaki, T., Aizaki, H., Ohkawa, K. and Suzuki, T. (2003) CYP3A4 inducible model for in vitro analysis of human drug metabolism using a bioartificial liver. Hepatology 37, 665–673

30 Mangelsdorf, D. J. and Evans, R. M. (1995) The RXR heterodimers and orphan receptors. Cell 83, 841–850

31 Chambon, P. (1996) A decade of molecular biology of retinoic acid receptors. FASEB J 10, 940–954

32 Friedman, A. D., Landschulz, W. H. and McKnight, S. L. (1989) CCAAT/enhancer binding protein activates the promoter of the serum albumin gene in cultured hepatoma cells. Genes Dev. 3, 1314–1322

33 Trautwein, C., Rakemann, T., Pietrangelo, A., Plümpe, J., Montosi, G. and Manns, M. P. (1996) C/EBP-β/LAP controls down-regulation of albumin gene transcription during liver regeneration. J. Biol. Chem. 271, 22262–22270

34 Ossipow, V., Descombes, P. and Schibler, U. (1993) CCAAT/enhancer-binding protein mRNA is translated into multiple proteins with different transcription activation potentials. Proc. Natl. Acad. Sci. U.S.A. 90, 8219–8223

35 Calkhoven, C. F., Müller, C. and Leutz, A. (2000) Translational control of C/EBPα and C/EBPβ isoform expression. Genes Dev. 14, 1920–1932

36 Lin, F. T., MacDougald, O. A., Diehl, A. M. and Lane, M. D. (1993) A 30-kDa alternative translation product of the CCAAT/enhancer binding protein α message: transcriptional activator lacking antimitotic activity. Proc. Natl. Acad. Sci. U.S.A. 90, 9606–9610

37 Descombes, P. and Schibler, U. (1991) A liver-enriched transcriptional activator protein, LAP, and a transcriptional inhibitory protein, LIP, are translated from the same mRNA. Cell 67, 569–579

38 Baldwin, B. R., Timchenko, N. A. and Zahnow, C. A. (2004) Epidermal growth factor receptor stimulation activates the RNA binding protein CUG-BP1 and increases expression of C/EBPβ-LIP in mammary epithelial cells. Mol. Cell. Biol. 24, 3682–3691

39 Calkhoven, C. F., Bouwman, P. R., Snippe, L. and Ab, G. (1994) Translation start site multiplicity of the CCAAT/enhancer binding protein α mRNA is dictated by a small 5′ open reading frame. Nucleic Acids Res. 22, 5540–5547

40 Wang, N. D., Finegold, M. J., Bradley, A., Ou, C. N., Abdelsayed, S. V., Wilde, M. D., Taylor, L. R., Wilson, D. R. and Darlington, G. J. (1995) Impaired energy homeostasis in C/EBPα knockout mice. Science 269, 1108–1112

41 Poli, V. (1998) The role of C/EBP isoforms in the control of inflammatory and native immunity functions. J. Biol. Chem. 273, 29279–29282

42 Wang, H., Iakova, P., Wilde, M., Welm, A., Goode, T., Roesler, W. J. and Timchenko, N. A. (2001) C/EBPα arrests cell proliferation through direct inhibition of Cdk2 and Cdk4. Mol. Cell 8, 817–828

43 Jover, R., Bort, R., Gómez-Lechón, M. J. and Castell, J. V. (2002) Down-regulation of human CYP3A4 by the inflammatory signal interleukin 6: molecular mechanism and transcription factors involved. FASEB J. 16, 1799–1801

44 Welm, A. L., Mackey, S. L., Timchenko, L. T., Darlington, G. J. and Timchenko, N. A. (2000) Translational induction of liver-enriched transcriptional inhibitory protein during acute phase response leads to repression of CCAAT/enhancer binding protein α mRNA. J. Biol. Chem. 275, 27406–27413

45 Hsu, W. and Chen-Kiang, S. (1993) Convergent regulation of NF-IL6 and Oct-1 synthesis by interleukin-6 and retinoic acid signaling in embryonal carcinoma cells. Mol. Cell. Biol. 13, 2515–2523

46 Hsieh, C. C., Xiong, W., Xie, Q., Rabek, J. P., Scott, S. G., An, M. R., Reisner, P. D., Kuninger, D. T. and Papaconstantinou, J. (1998) Effects of age on the posttranscriptional regulation of CCAAT/enhancer binding protein α and CCAAT/enhancer binding protein β isoform synthesis in control and LPS-treated livers. Mol. Biol. Cell 9, 1479–1494

47 Timchenko, N. A., Welm, A. L., Lu, X. and Timchenko, L. T. (1999) CUG repeat binding protein (CUGBP1) interacts with the 5′ region of C/EBPβ mRNA and regulates translation of C/EBPβ isoforms. Nucleic Acids Res. 27, 4517–4525

48 Timchenko, L. T., Iakova, P., Welm, A. L., Cai, Z. J. and Timchenko, N. A. (2002) Calreticulin interacts with C/EBPα and C/EBPβ mRNAs and represses translation of C/EBP proteins. Mol. Cell. Biol. 22, 7242–7257

49 Welm, A. L., Timchenko, N. A. and Darlington, G. J. (1999) C/EBPα regulates generation of C/EBPβ isoforms through activation of specific proteolytic cleavage. Mol. Cell. Biol. 19, 1695–1704

50 Lichtsteiner, S. and Schibler, U. (1989) A glycosylated liver-specific transcription factor stimulates transcription of the albumin gene. Cell 57, 1179–1187

VIROLOGY

ELSEVIER

Down-regulation of the internal ribosome entry site (IRES)-mediated translation of the hepatitis C virus: Critical role of binding of the stem-loop IIId domain of IRES and the viral core protein

Takashi Shimoike [a,*], Chika Koyama [a], Kyoko Murakami [b], Ryosuke Suzuki [b],
Yoshiharu Matsuura [c], Tatsuo Miyamura [a,b], Tetsuro Suzuki [b,*]

[a] *Department of Virology II, National Institute of Infectious Diseases, Musashi-murayama, Tokyo 208-0011, Japan*
[b] *Department of Virology II, National Institute of Infectious Diseases, Shinjuku-ku, Tokyo 162-8640, Japan*
[c] *Research Center for Emerging Infectious Diseases, Research Institute for Microbial Diseases, Osaka University, Suita-shi, Osaka 565-0871, Japan*

Received 27 May 2005; returned to author for revision 1 July 2005; accepted 7 October 2005
Available online 17 November 2005

Abstract

In a previous study, we observed that hepatitis C virus (HCV) core protein specifically inhibits translation initiated by an HCV internal ribosome entry site (IRES). To investigate the mechanism by which down-regulation of HCV translation occurs, a series of mutations were introduced into the IRES element, as well as the core protein, and their effect on IRES activity examined in this study. We found that expression of the core protein inhibits HCV translation possibly by binding to a stem-loop IIId domain, particularly a GGG triplet within the hairpin loop structure of the domain, within the IRES. Basic-residue clusters located at the N-terminus of the core protein have an inhibitory effect on HCV translation, and at least one of three known clusters is required for inhibition. We propose a model in which competitive binding of the core protein for the IRES and 40S ribosomal subunit regulates HCV translation.
© 2005 Elsevier Inc. All rights reserved.

Keywords: Hepatitis C virus; Internal ribosome entry site; Translation; Core protein

Introduction

Hepatitis C virus (HCV) is a major causative agent of chronic hepatitis, liver cirrhosis, and hepatocellular carcinoma (Alter and Seeff, 2000; Pawlotsky, 2004). HCV contains approximately 9.6 kb of positive-strand RNA with one open reading frame encoding a precursor polyprotein, which is proteolytically cleaved to produce the mature structural and non-structural proteins of HCV (Choo et al., 1991. Grakoui et al., 1993 Hijikata et al., 1991, Takamizawa et al 1991). Although HCV exhibits considerable genetic diversity, the 5′ untranslated region (5′UTR) of the viral genome is relatively well conserved among all genotypes.

HCV translation is initiated by a cap-independent mechanism involving an internal ribosome entry site (IRES), comprising nearly the entire 5′UTR of the genome. There is evidence to suggest that the first 12 to 30 nucleotides (nt) of the coding sequence are also important for IRES activity (Hellen and Pestova. 1999; Lu and Wimmer. 1996; Reynolds et al., 1995). The proposed secondary structure of the HCV 5′UTR, thought to contain four major domains (I to IV) (Fig. 1), may be conserved among HCV and related flaviviruses and pestiviruses (Brown et al. 1992 Honda et al. 1999a. 1999b: Zhao and Wimmer. 2001).

Recruitment of the 43S ribosomal complex, containing a small 40S ribosomal subunit, eukaryotic initiation factor (eIF) 3, and a tRNA–eIF2–GTP ternary complex, to mRNA molecules is critical for initiation of eukaryotic protein synthesis. The 40S subunit and eIF3 can bind independently to the HCV IRES (Bura 1 99 H(len a d Pest 999 K cfi 00 S o a et a 998). However, it appears that interaction between IRES RNA and the 40S

* Corresponding authors. T Shimoike is to be contacted at fax: +81 42 561 4729. T Suzuki. fax: +81 3 5285 1161
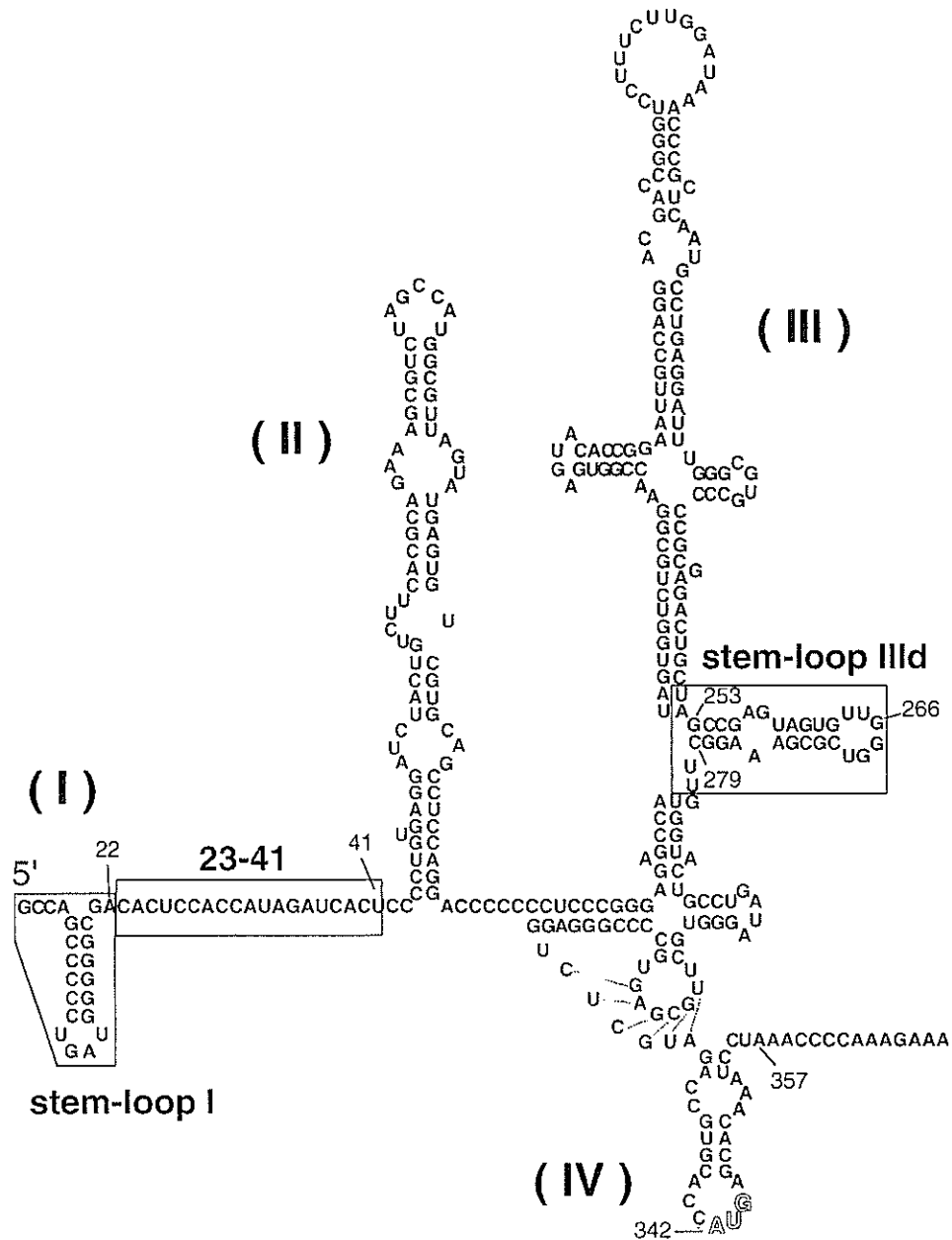*E-mail addresses:* shimoike@nih.go.jp (T Shimoike), tesuzuki@nih.gi.jp (T. Suzuki).

Fig. 1 Predicted secondary structure of the HCV 5'UTR (Honda et al. 1999a, 1999b). The stem-loop I, nt 23–41, and stem-loop IIId domains are highlighted. The initiator AUG codon is shown in the sequence of loop IV. Small numerals indicate the nucleotide positions from the 5'end.

subunit drives formation of the IRES-40S subunit–eIF3 complex since HCV IRES RNA demonstrates similar affinity for the 40S subunit and the 40S–eIF complex (Kie 2001). Other cellular factors such as La autoantigen (2000. Ali and Siddiqi 90' m; e '9), heterogeneous ribonucleoprotein L (Hahm et a '), poly-C binding protein (Fukushi e. al 200i Span Schwartz. 1999), and pyrimidine tract-binding protein (h and Siddiqui. 1995. Anwar et a '000) also bind to the IRES element and modulate translation.

HCV core protein, which is located at the N-terminus of the viral polyprotein, is a putative nucleocapsid protein given the basic nature of its amino acid (aa) residues and the organization of the HCV genome. HCV core protein can form multimeric complexes, as well as heterodimer complexes with envelope E1 protein (Lo et 996). Physical interaction between the core protein and viral genomic RNA is thought to occur during nucleocapsid formation. The results of several Northwestern analyses suggest that the core protein binds to the 5'UTR of the HCV genome, regardless of the specific RNA sequences involved (Santolini et al 994 H ig et 995 Ha al. 1999). We previously used both in vivo and in vitro systems to demonstrate that the core protein preferentially binds to positive-stranded viral RNA containing the 5'UTR and

part of the structural protein-coding region (Shimoike et al., 1999). In addition, the core protein has a high affinity for the stem-loop IIId domain of the 5′UTR (Fig. 1) and for (G)-rich nucleotides (Tanaka et al., 2000).

In addition, evidence regarding the importance of the interaction between HCV core protein and HCV RNA in regulating viral translation is accumulating. We previously reported that expression of the core protein down-regulates HCV translation through interaction(s) involving 5′ regions of the viral genome (Shimoike et al., 1999). Although some evidence suggesting inhibition of HCV translation through RNA–RNA interactions, rather than core–RNA interactions, exists (Wang et al., 2000; Kim et al., 2003), several studies indicate that the core protein modulates HCV translation. Specifically, regions of the core protein corresponding to aa 34–44 (Zhang et al., 2002) or aa 1–20 (Li et al., 2003) are important for inhibition of HCV translation. The core protein may down- or up-regulate HCV IRES activity in a dose-dependent manner (Boni et al., 2005).

The aim of the present study was (1) to clarify the nature of interaction between the HCV core protein and the viral IRES element and (2) to gain insight into the relationship between core protein-mediated inhibition of translation and core–IRES interactions using a combination of techniques, including an in vivo reporter assay and in vitro surface plasmon resonance (SPR) analysis.

Results

Effect of the core protein-coding sequence on HCV IRES-initiated translation

Since there is conflicting data regarding the effect of the core protein or the core protein sequence on HCV IRES-directed translation (Shimoike et al., 1999; Zhang et al., 2002; Li et al., 2003; Boni et al., 2005), we sought to determine whether the RNA sequence of the core-coding region inhibits HCV IRES activity in the present experiment. A single substitution replacing A with U at nt 357 was introduced to produce a stop codon near the 5′ end of the region encoding the core protein, as previously described (Wang et al., 2000). This mutant, known as pCAGFS, produces core protein RNA with a single substitution, resulting in a core peptide, five residues in length, encoded by the N-terminal. Western blot analysis was then used to confirm that the core protein is not expressed by HepG2 cells following transfection with pCAGFS (Fig. 2C). RNA molecules transcribed in vitro from two reporter plasmids, HCVLuc and RLuc, expressing firefly luciferase (FL) controlled by the IRES of HCV genotype 1b and Renilla luciferase (RL) controlled by a cap-dependent mechanism, respectively, were cotransfected into cells after 48 h of transfection with pCAGFS39 or core-expressing pCAGC191 (Suzuki et al., 2001). Cell lysate samples were prepared 6 h post-reporter transfection and assayed for expression of both luciferases. As shown in Fig. 2A, the translational activity of HCV IRES was reduced in cells expressing the core protein, but not in cells transfected with
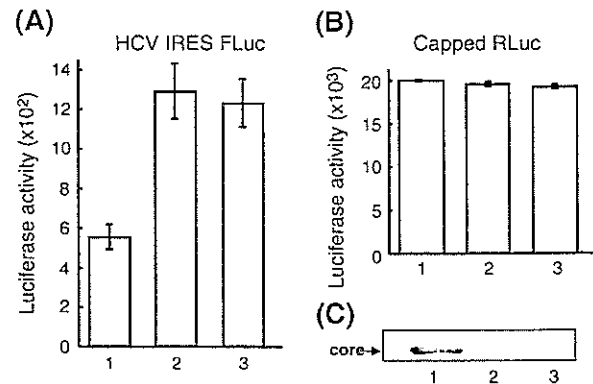

Fig. 2. Effect of the core protein-coding sequence on the translation initiated by HCV IRES. HepG2 cells transfected with pCAGC191 (lane 1), pCAGFS (lane 2), or pCAGGS (lane 3) were cotransfected with reporter RNAs of HCVLuc and the capped RLuc. The activities of both FL (A) and RL (B) were measured by a luminometer. The activities of both FL and RL were determined in at least three independent experiments, each of which conduced with triplicate samples. (C) Western blot analysis of the core protein expressed in the infected cells.

pCAGFS, indicating that the HCV core protein, but not the core-coding sequence, inhibits HCV IRES-directed translation. Transfection with neither core-expressing or non-expressing constructs modulated cap-dependent translation (Fig. 2B).

Effect of partial deletion of the HCV 5′UTR on inhibition of viral IRES-mediated translation by the core protein

In previous studies, we demonstrated that purified HCV core protein binds most efficiently and stably to the stem-loop IIId domain of the 5′UTR of HCV RNA followed by the stem-loop I domain and the region encoding nt 23–41 (Fig. 1; Tanaka et al., 2000). In addition, we revealed that the core protein expressed in HepG2 cells inhibits the IRES-dependent translation of HCV (Shimoike et al., 1999). It can be hypothesized that binding of the core protein to one or more regions of the 5′UTR might inhibit translation. To address this issue, we constructed three reporter plasmids: ΔILuc, Δ23–41Luc, and ΔIIIdLuc, with deletions of domain 1 (Δ1–22), nt 23–41, and domain IIId (Δ254–278) of the HCV 5′UTR, respectively, also containing the FL gene (Fig. 3A). RNA molecules transcribed from these reporter plasmids in vitro were transfected into HepG2 cells, after which luciferase activity within the cell lysate samples was analyzed. Consistent with previous reports, deletions of domain I (ΔIluc) (Luo et al 2003; Friebe et al 2001) or IIId (ΔIIIdLuc) (Jubin et al 2000) profoundly impaired IRES activity, with a >95% reduction in activity (data not shown), thus demonstrating the importance of these loop structures for HCV translation. Therefore, in the following experiment, we adjusted the dose of each reporter transcript to ensure a consistent level of FL expression.

To investigate the effect of the core protein on translation mediated by wild-type or mutated HCV 5′UTR as described above, cells infected with a recombinant baculovirus carrying
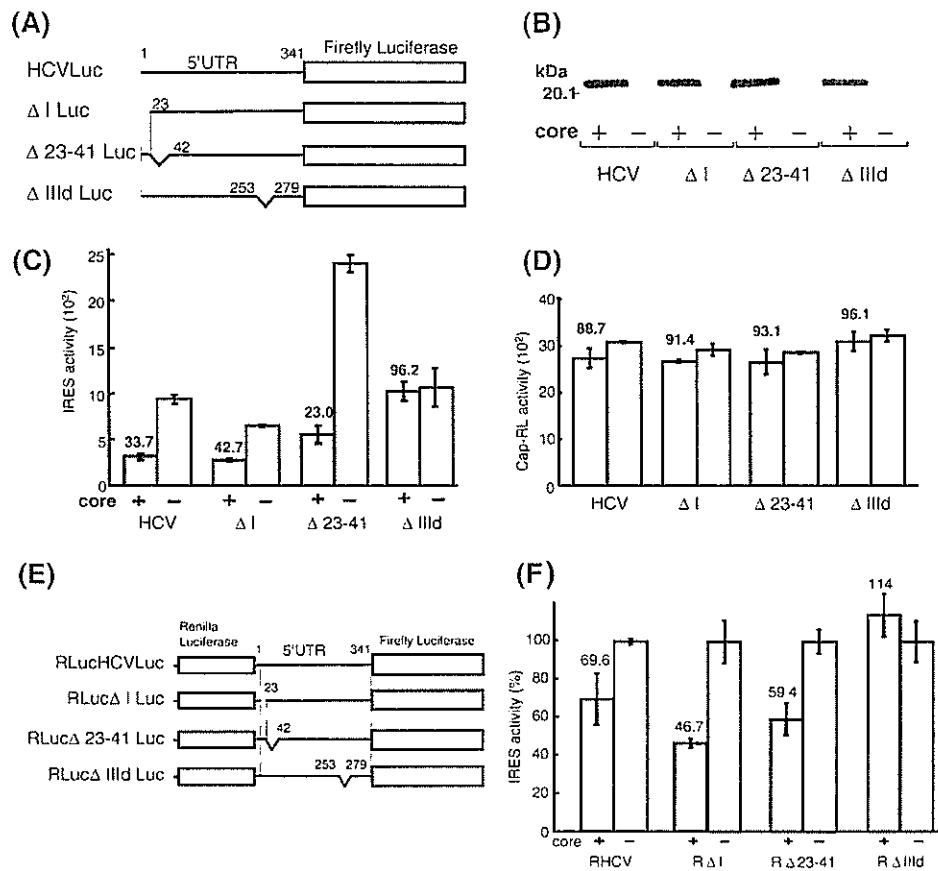
Fig. 3. Effect of deletion mutations in HCV 5′UTR on inhibition of the viral IRES-mediated translation by the core protein. HepG2 cells infected with AcCA39 or AcCAG at a multiplicity of infection of 20 were transfected with monocistronic wild-type (HCVLuc) or deletion mutants (ΔILuc, Δ23–41Luc, ΔIIIdLuc) of reporter RNAs together with the capped RLuc RNA or transfected with bicistronic wild-type (RLucHCVLuc) or deletion mutants (RLucΔILuc, RLucΔ23–41Luc, RLucΔIIIdLuc) of reporter RNAs. The activities of both FL and RL were determined in at least three independent experiments, each of which conduced with triplicate samples. Schematic representation of the monocistronic and bicistronic deletion mutants used in this study is shown in panels A and E, respectively. (B) Western blot analysis of the core protein in each cell lysate in which the luciferase activities were measured. (C) Relative luciferase activities were normalized with those of RLuc. (D) The activities of RLuc in cells cotransfected with RLuc and HCVLuc or deletion mutants are shown. (F) HCV IRES activity was determined by calculating the abundance of Fluc relative to RLuc, with that of each reporter in the absence of the core protein normalized to 100%. Mean values with standard deviations were indicated.

the entire HCV core gene (AcCA39; Shimoike et al., 1999) or an empty vector (AcCAG) were cultured for 2 days, followed by transfection with reporter transcripts, either wild-type HCVLuc (0.1 μg/well), ΔILuc (6 μg/well), Δ23–41Luc (0.2 μg/well), or ΔIIIdLuc (6 μg/well), together with capped RLuc RNA (0.08 μg/well). As indicated in Fig. 3C, expression of the core protein inhibited HCV IRES-mediated translation from ΔILuc and Δ23–41Luc, as well as from HCVLuc, by more than 50%. In contrast, inhibition of translation by the core protein was not observed in cells transfected with ΔIIIdLuc. As shown in Fig. 3D, the expression of neither the core protein nor any of the IRES-directed reporters influenced cap-directed translation. Thus, as previously demonstrated (Shimoike et al., 1999), RL activity was used as an internal control to normalize the efficiency of transfection in the following experiments (Figs. 4 and 6). Western blotting was used to confirm that core protein concentrations within the cell lysate of cells infected with AcCA39 were comparable in the presence of each of the reporter RNA molecules (Fig. 3B). We observed a similar

effect of the core protein on HCV IRES activity when equal amounts (6 μg/well) of each HCVLuc, ΔILuc, Δ23–41Luc, or ΔIIIdLuc transcript were transfected (data not shown). These results eliminate the possibility that there is no translational inhibition because the core protein is destabilized in cells transfected with ΔIIIdLuc RNA. We also determined the effect of the core protein on HCV translation initiated from bicistronic reporters: RLucHCVLuc (wild-type), RLucΔILuc (deletion of domain I), RLucΔ23–41Luc (deletion of nt 23–41), and RLucΔIIIdLuc (deletion of domain IIId) (Fig. 3E). Consistent with results obtained from the monocistronic constructs, expression of the core protein showed an inhibitory effect on HCV translation mediated by RLucHCVLuc, RLucΔIluc, or RLucΔ23–41Luc, but not by RLucΔIIIdLuc (Fig. 3F). The capped RL activity from each reporter was similar and was not influenced by expression of the core protein (data not shown). These results suggest that the stem-loop IIId domain of the 5′UTR is important for inhibition of HCV translation by the core protein.
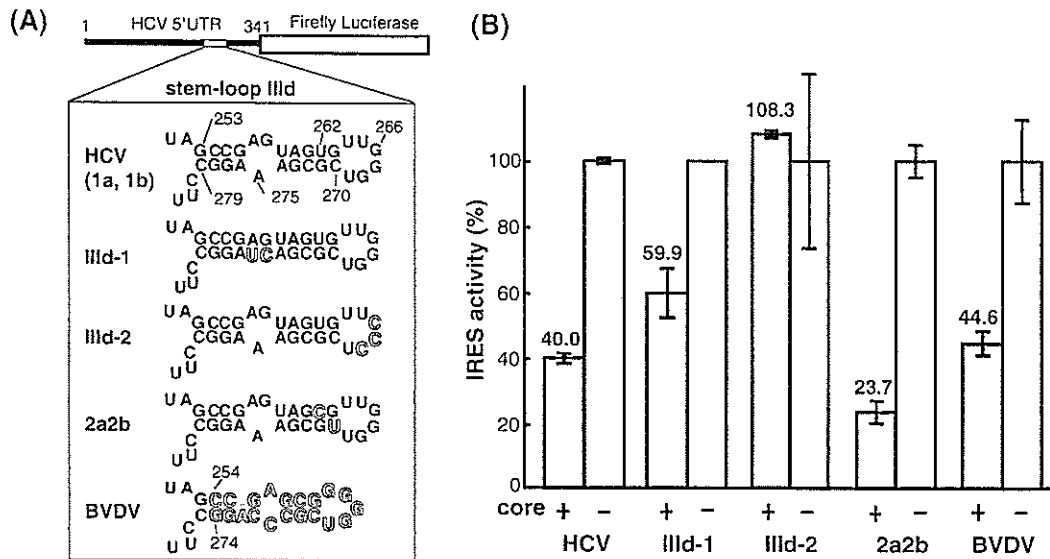
Fig. 4. Mutational analysis of the stem-loop IIId domain. (A) Schematic representation of the predicted secondary structures of the IIId domain of mutated reporters used in this study. (B) The core protein and luciferase reporters are expressed as described in the legend to Fig. 3, except reporters indicated. HCV IRES activity was determined and presented as described in the legend to Fig. 3C.

Mutational analysis of the stem-loop IIId domain

To further investigate the functional role of the stem-loop IIId domain (nt 253–279) in core protein-mediated inhibition of HCV translation, we engineered stem-loop IIId domains with the following four mutations (Fig. 4A): (1) IIId-1Luc, in which the A at nt 275 was changed to UC, thus forming a double-stranded structure instead of a bulge loop in the IIId, (2) IIId-2Luc, in which the GGG triplet (nt 266–268) was changed to a CCC triplet within the loop of stem-loop IIId, (3) 2a2bLuc, in which the U at nt 262 and the C at nt 270 were changed to C and U, respectively, thus changing the genotype to 2a/2b, and (4) BVDVLuc, in which the stem-loop IIId (nt 254–274) sequence was changed to that of bovine viral diarrhea virus (BVDV)-1. Cells that did or did not express the core protein were transfected with each of the above described reporter RNA transcripts, after which luciferase activity was measured. As shown in Fig. 4B, IIId-2Luc, containing a mutation of the GGG triplet of the apical loop, demonstrated no inhibition of HCV IRES-mediated translation by the core protein, whereas IIId-1Luc, containing a mutation within the bulge loop structure, showed only a marginally reduced inhibitory effect of the core protein. We previously demonstrated that HCV core protein binds most efficiently to (1) the stem-loop IIId domain, compared to other structural domains of the 5′UTR, and to (2) G octamer (G_8), as opposed to A_8, C_8, and U_8, using a quantitative SPR method (Tanaka et al 2000). Thus, the results obtained here suggest that the apical loop is a critical recognition site for translational inhibition by the core protein. It is likely that the inhibitory activity of the core protein on HCV IRES-mediated translation is related to its efficiency of RNA binding.

We also observed the core protein to exert an inhibitory effect on translation directed by either 2a2bLuc or BVDVLuc,

similar to that observed with wild-type HCVLuc, involving a 5′UTR sequence of genotype 1. Since the IIId domain sequence of HCVLuc is conserved among genotypes 1, 3, 4, and 5 and since that of 2a2bLuc is shared with genotype 6, it appears that inhibition of HCV translation by the core protein is independent of the viral genotype and occurs in most HCV isolates. Sequence alignment of HCV and various pestiviruses showed that, although the primary nucleotide sequence of the IIId domain exhibits considerable variability, the predicted secondary structure of the domain is highly conserved among these viruses as reviewed previously (Rijnbrand and Lemon. 1999). Furthermore, the GGG triplet followed by U at the apical loop and one bulge loop in the domain are well conserved among HCV and pestiviruses. These suggest that the nucleotide sequence of the apical loop, particularly the GGG triplet, is more important than the stem-structure sequence of the IIId domain for core protein-mediated translational inhibition.

Relationship between translational inhibition and ability of the core protein to bind to the IIId domain within the 5′UTR

To investigate the relationship between inhibition of HCV translation by the core protein and ability of the core protein to bind to IIId RNA, we prepared two biotinylated oligo RNA molecules, IIId-1 and IIId-2 (nt 251–282), containing identical mutations in the bulge and apical loops of their IIId domains as the mutated reporters IIId-1Luc and IIId-2Luc, respectively (F   ,A). These mutant or wild-type oligo RNA (IIId-wt) molecules were then coupled to streptavidin-coated sensor chips and allowed to bind to purified recombinant core protein. The results of subsequent SPR analysis using a BIAcore biosensor are shown in Fig 5. The core protein was observed to bind to IIId-1 RNA as efficiently as to IIId-wt RNA,
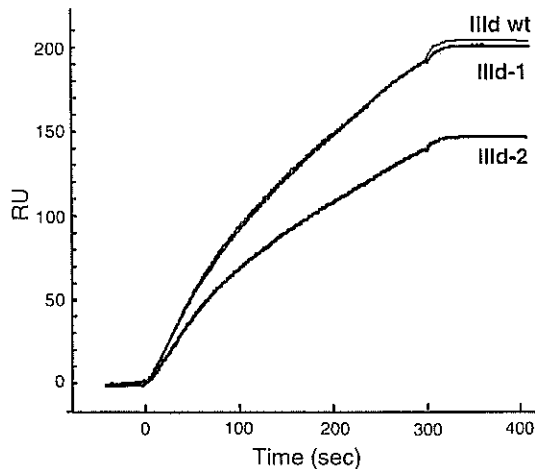
Fig. 5. Binding of the core protein to oligo RNAs corresponding to the mutated IIId domains. The real time binding between the core protein and wild-type (IIId wt) or mutants (IIId-1 and IIId-2) of the stem-loop IIId was examined. Biotinylated oligonucleotides were immobilized of the streptavidin pre-coated sensor chips followed by being exposed to 40 μl of the solution containing the core protein (4 μg/ml) with a flow rate of 8 μl/min. The sample flow was stopped, and the buffer washout began at 300 s. The amounts of immobilized synthetic oligonucleotides, IIId-wt, IIId-1, and IIId-2 were 211.0, 206.9, and 212.4 resonance units, respectively.

suggesting that RNA mutations disrupting the bulge loop structure have little or no effect on binding of the core protein. In contrast, a marked reduction in binding affinity of the core protein for mutant IIId-2 RNA was observed. As a negative control, we found that the core protein does not bind to oligo RNA corresponding to IIIe or IIIf domain (data not shown; Tanaka et al., 2000). It is likely that the apical loop sequence and/or the GGG triplet are important for RNA binding of the core protein, which is consistent with prior observations suggesting that the core protein binds to G-stretch sequence(s) with high affinity.

Combined with the data shown in Fig. 4B, the inhibitory effect of the core protein on HCV IRES activity correlates well with its ability to bind to wild-type and mutated IIId RNA. In light of the observation that the IIId domain is important for IRES activity and from suggestion that the domain IIId interacts with 40S (Otto et al., 2002; Jubin et al., 2000; Lukavsky et al., 2000; Spahn et al., 2001), the HCV core protein may inhibit viral IRES-dependent translation by preventing required interactions between RNA molecules and the 40S by binding to the IRES sequence including the apical loop of the IIId domain.

Role of basic-residue clusters within the core protein in inhibition of HCV translation

The amino-terminal portion of the core protein is able to bind to viral nucleic acids (Santolini et al., 1994). This region contains three clusters of arginine- and lysine-rich sequences (aa 5–13, 38–43, and 58–71). To investigate the role of these basic-residue clusters in inhibition of HCV translation by the core protein, we constructed a series of core mutants, in which lysine and arginine residues within one or more of the basic-residue clusters of the core protein were substituted with alanine residues, as depicted in Fig. 6A. Two days after transfection with either wild-type (pCAGC191) or core mutant (pCAGC191m1–m7) constructs, the cells were cotransfected with HCVLuc and capped-RLuc RNA. As indicated in Fig. 6B, core mutants containing alanine substitutions within one or two clusters (C191m1, m2, m3, m4, m5, and m6) retained the ability to inhibit HCV IRES-mediated translation, similar to the wild-type core protein. However, a core mutant with alanine substitutions involving all three clusters, C191m7, demonstrated little to no inhibition of translation. Expression of the core protein in each transfectant was determined by Western blotting (Fig. 6C), and none of the mutants influenced cap-dependent translation (data not shown). These results
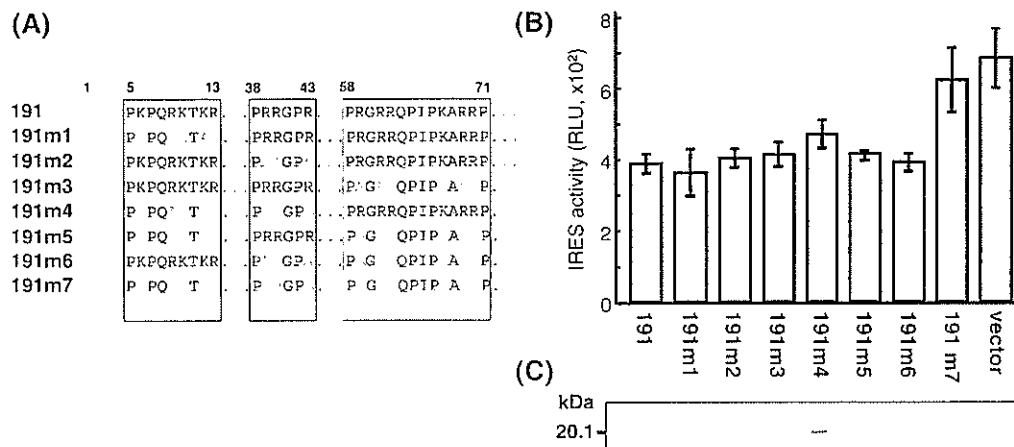

Fig. 6. A role of basic-residue clusters within the core protein in inhibition of the HCV translation. (A) Schematic representation of the mutated core proteins substituted in three basic aa clusters. Lysine or arginine residues substituted with alanine in the clusters are shown with outlined letters. (B) Two days after the transfection with either wild-type (191) or mutated (191m1–m7) core-expressing constructs, HepG2 cells were further cotransfected with HCVLuc and capped-RLuc RNAs. Relative luciferase activities (RLU) were determined as described in Materials and methods and the legend to Fig (C) The amounts of the wild-type and mutant core proteins expressed in HepG2 cells are shown by Western blotting.

suggest that all three basic-residue clusters of the core protein can mediate inhibition of HCV translation and that at least one cluster is required for inhibition.

Discussion

In this study, we investigated the mechanism by which the core protein modulates HCV IRES activity using an in vivo reporter assay and SPR technology. We demonstrated the importance of a stem-loop IIId domain, spanning nt 253–279, in core protein-mediated inhibition of HCV IRES-mediated translation. In a previous study, we demonstrated preferential binding of the core protein to domain IIId of the 5′UTR followed by domain I and a region spanning nt 23–41 (Fig. 1), upon examining 10 oligonucleotides corresponding to various structured domains of the viral 5′UTR (Tanaka et al., 2000). The core protein did not have an inhibitory effect on translation directed by mutated IRES lacking the IIId domain. However, translation initiated by IRES mutants with deletions of domain I or nt 23–41 was significantly inhibited by the core protein to a similar extent as wild-type IRES-mediated translation (Fig. 3B). Further mutational analysis was then used to determine whether specific IIId nucleotide sequences were important for inhibition of translation by the core protein. We determined that the GGG triplet (nt 266–268) within the IIId apical loop was most critical for core protein-mediated inhibition (Fig. 4B). Combined with the results of SPR analysis (Fig. 5), the data presented here suggest that inhibition of HCV IRES-directed translation by the core protein depends on the binding efficiency of the core protein for the viral IRES element.

Domain III, which is composed of six distinct regions containing stem-loop structures, forms the core of the HCV IRES and is essential for viral translation. Previous studies suggest that domain III plays a role in recruiting the 40S ribosomal subunit and eIF3 by direct interaction with stem-loops IIId/e/f and IIIb, respectively, even though the 40S subunit makes multiple interactions with the IRES and also binds to stem-loop II and the pseudoknot domain of the IRES element (Kieft et al., 2001, Kolupaeva et al., 2000; Sizova et al., 1998). Stem-loop IIId is a highly conserved region within domain III in most HCV isolates, consisting of two double-stranded helical elements separated by a 3-nt internal asymmetric loop with a 6-nt hairpin loop at the distal end of each helical region. IRES sequence deletions, including deletion of stem-loop IIId, as well as point mutations, inhibit binding of the 40S subunit and IRES function (Rijnbrand et al., 1995; Honda et al., 1996; Kieft et al., 1999). Specifically, substitution mutations of the GGG triplet within the IIId apical loop region produce significant loss of IRES activity, as well as alterations in RNA folding, indicating that the GGG triplet is a critical region for HCV translation (Kieft et al. 99; Jub al 2000). In addition, antisense 2′-O-methyloligonucleotides targeted to the IIId domain are known to compete with the 40S subunit for binding and to inhibit viral translation (Ta let-Lopez et al. 2003). Moreover, the secondary structure of the IIId domain is important for binding of the S9 ribosomal protein (Odreman-Macchioli et al., 2000). Consistent with

these observations, we also observed that deletion of the IIId domain (ΔIIIdLuc), or a G-to-C substitution within the GGG triplet (IIId-2Luc), significantly reduced IRES activity.

Although the sequence of the IIId domain is highly conserved, sequence polymorphism of the helical region exists among the six major genotypes. With regard to nt 262 and nt 270 of the IIId domain, genotypes 1, 3, 4, and 5 of HCV encode U (nt 262) and C (nt 270), respectively. On the other hand, genotypes 2 and 6 encode C (nt 262) and U (nt 270), respectively. We observed that translation directed by the IRES sequence of genotypes 2 and 6 (2a2bLuc) was more efficient than that directed by the IRES sequence of genotypes 1, 3, 4, and 5 (HCVLuc) (Fig. 4B). Previous studies also demonstrated differences in the efficiency of IRES activity among different HCV genotypes and suggest that the 5′UTR of genotype 2(b) has the most marked IRES activity (Tsukiyama-Kohara et al., 1992; Kamoshita et al., 1997; Collier et al., 1998). Thus, sequence polymorphism involving the helical region of IIId might explain the observed variability in IRES activity when comparing the 5′UTR sequences of different HCV genotypes. Expression of the core protein inhibits HCV translation directed by 2a2bLuc to a similar or same extent as that directed by HCVLuc. This finding suggests that inhibition of viral translation by the core protein commonly occurs during the HCV life cycle and is not limited to certain genotypes. The deletion of the 5′-proximal stem-loop domain I (ΔILuc) significantly reduced IRES activity (data not shown), although the ability of the core protein to inhibit translation was retained (Fig. 3B). Published data regarding the role of domain I in inhibition of HCV translation are not consistent. Some researchers suggest that the 5′-proximal region containing domain I is not essential for HCV IRES activity (Honda et al., 1996; Kamoshita et al., 1997). However, other researchers suggest that this stem-loop element is required for optimal IRES-mediated HCV translation (Friebe et al., 2001, Fukushi et al., 1994; Luo et al., 2003). We compared HCV IRES activity mediated by monocistronic and bicistronic reporters with deletion of domain I and found that an inhibitory effect of the domain I deletion observed from the bicistronic reporter was less evident than that from the monocistronic one: the reduction in IRES activity caused by the deletion was 95% and 40% for the monocistronic and bicistronic constructs, respectively. Although similar trends were observed in the previous studies using cultured cells (Friebe et al. 2001 Luo et al. 2003; Kamoshita et al 1997), in vitro transcription/translation studies demonstrated that the translational efficiency of the reporters deleted with domain I is higher than that of the wild-type (H· ic al 1996; Kamoshita al 99?). It may be likely that differences in (1) gene constructs such as mono-cistronic and bicistronic reporters and (2) host cell conditions influence such inconsistent observations.

HCV core protein is highly basic, especially its N-terminal half, and it is thought to encapsulate the viral genome within a viral nucleocapsid. The RNA-binding domain of the core protein has been mapped to 75 aa residues within the N-terminal, in which three clusters of highly arginine/lysine-rich sequences are well conserved among HCV isolates (Santolini et

al., 1994). We previously observed preferential binding between the core protein and positive-stranded HCV RNA spanning the 5′UTR and part of the structural-protein coding region (nt 1–2327) (Shimoike et al., 1999). In this study, we demonstrated the importance of three basic aa residue clusters within the N-terminal region of the HCV core protein for its inhibitory effect on viral IRES activity. At least one cluster is required for inhibition of translation by the core protein. Previous studies with a series of deletion mutants suggest that aa 34–44 (Zhang et al., 2002) or aa 1–20 (Li et al., 2003) within the core protein are crucial for inhibition of translation initiated by HCV IRES. To investigate the contribution of these basic-residue-rich domains within the core protein to inhibition of viral translation, we employed substitution mutagenesis of the full-length core protein in order to reduce the occurrence of conformational changes in the core protein due to the introduction of mutations.

Although an increasing body of evidence shows involvement of the core protein in translational regulation, there are conflicting data regarding the exact mechanism by which this occurs. In contrast to studies describing direct inhibition of HCV translation by expression of the core protein (Shimoike et al., 1999; Zhang et al., 2002; Li et al., 2003), a recent report suggests that the core protein modulates HCV IRES function in a dose-dependent manner, with low amounts of the core protein producing up-regulation and greater amounts resulting in down-regulation (Boni et al., 2005). The core protein does not only inhibit translation initiated by the HCV IRES, but also cap-dependent translation and translation initiated by encephalo-myocarditis virus (EMCV) IRES (Li et al., 2003). In an earlier study, neither cap- nor EMCV IRES-dependent translation were inhibited by expression of the core protein (Shimoike et al. 1999). Other studies suggest that the core protein-coding sequence, but not the core protein itself, modulates HCV IRES function, through a long-range RNA–RNA interaction (Wang et al., 2000; Kim et al., 2003). In the present experiment, however, down-regulation of HCV IRES-directed translation by the core protein-coding RNA sequences was eliminated by introducing a base-substitution mutation into the N-terminus of the core sequence in order to create a termination codon (Fig. 2). These contradictory findings might be due to different experimental conditions, such as the use of different reporter systems and host cells, as well as different levels of core protein in the assays used. To investigate the effect of the core protein on HCV IRES-dependent translation, we employed in vivo RNA transfection of monocistronic reporter constructs because HCV IRES is located at the 5′ end of the viral genome, and not internally, thus making it unnecessary to use a bicistronic reporter. Concerning bicistronic contexts, the possibility that the first cistronic sequence might influence IRES regulation directed by the second cistronic gene cannot be excluded. There is evidence to suggest that differences in translational regulation by the core protein might exist among different cell lines, including HepG2, Huh-7, and CV-1 cells (Wang et al. 2000; Li et al., 2003). We also observed differences between HepG2 and Huh-7 cells in terms of ability of the core protein to inhibit HCV IRES- and cap-dependent translation, which was not observed in Huh-7

cells (data not shown), as previously reported (Wang et al., 2000). Such cell-type specific effects might be related to differences in core protein expression since core protein expression by the recombinant baculovirus AcCA39 seems to be less abundant in Huh-7 cells, compared to HepG2 cells (data not shown). It is also possible that a cell-specific factor(s) are involved in translational regulation by the core protein. Thus, some interaction(s) between the highly ordered HCV IRES structure and/or the core protein and related host factors are likely cell-type-specific. Our previous report showed difference in the translation efficiency mediated by HCV IRES among human liver-derived cell lines, although the effect of the core protein on their translation was not determined (Aoki et al., 1998).

We performed the gel mobility shift assay to demonstrate the inhibition of the interaction between the HCV 5′UTR and the ribosome 40S subunit (40S). The complexes between purified 40S and the radiolabeled HCV 5′UTR (nt 1–330) were detected, and the amount of this band was decreased in the core protein-dose-dependent manner. In this condition, the core–5′UTR complex was competed with a non-labeled oligo RNA corresponding to IIId domain, but not with oligo RNAs of domain IV. However, the complex between the core protein and the 5′UTR was detected around the wells of the gel. To our knowledge, there has been no published data that in the gel mobility shift assay the core–5′UTR complex runs into the gel. Although these findings may support the idea that the core protein directly prevents binding of 40S to the HCV IRES, direct biochemical probing of the proposed interaction must wait for the advances in the protein chemistry of the HCV core protein.

Finally, based on the results of the present study and the existing literature, we propose a model of down-regulation of HCV translation mediated by the core protein (Fig. 7). In HCV-infected cells, the virus uncoats and releases its genomic RNA, which serves as a template for protein translation. Highly folded secondary and tertiary RNA elements in the 5′UTR function as cis signals for interaction with the 40S subunit and eIF3 during the initial process of HCV IRES-dependent translation. The high affinity interaction between HCV IRES and the 40S subunit is thought to be important for recruitment of the 43S particle to viral RNA, and the stem-loop IIId domain is a prerequisite for this interaction. Since the core protein binds most efficiently to the IIId domain in the HCV IRES element, it is relevant to note that the core protein may prevent an essential RNA–40S interaction by blocking the IIId domain, thereby reducing the viral translation efficiency. At an early stage of the HCV replication cycle, translation of the viral genome yields a polyprotein, which is subsequently processed to yield individual mature proteins. At a certain point, enough core protein is available to inhibit HCV translation by competing with the 40S subunit for IRES binding. Cells in which HCV translation is negatively controlled may have reduced levels of core protein due to its degradation by the ubiquitin/proteasome pathway (Suzuki et al. 2001 Moriishi et al. 2003), thereby decreasing the inhibitory effect of core protein. Thus, the core protein may
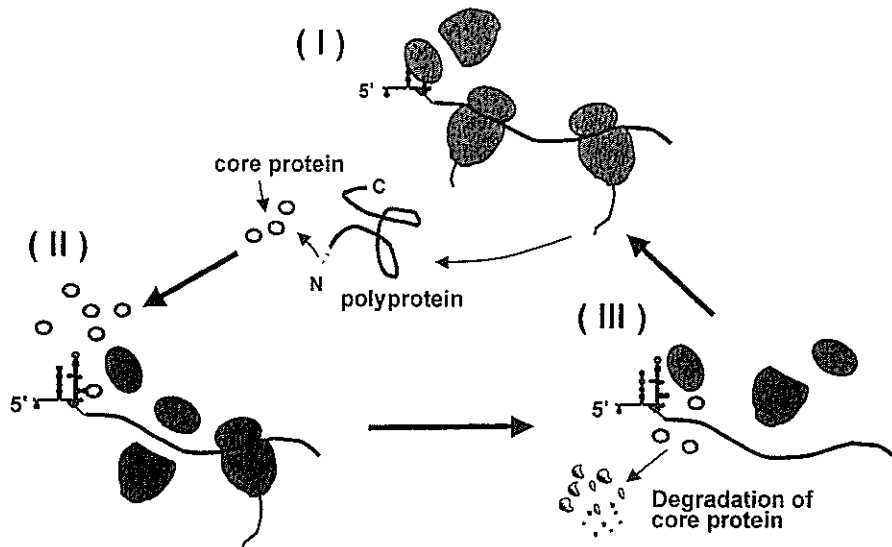
Fig. 7. Model for the regulation of HCV translation mediated by the core protein. Step 1: HCV translation is initiated through recognition of the 40S subunit and eIF3 by the IRES RNA tertiary structure. The viral polyprotein is expressed and processed into matured proteins, resulting in generation of the core protein. Step 2: The expressed core protein binds to the stem-loop IIId in the 5'UTR and inhibits the viral translation by competing with 40S subunit for binding to the IRES. Step 3: The reduced translational efficiency results in decreasing the levels of HCV proteins and replication. Degradation of the core protein through the ubiquitin/proteasome pathway may also contribute to reducing the amounts of the core protein in cells. A low concentration of the core protein possibly leads to recovery of the translational efficiency.

contribute, through its competitive interaction with the IRES IIId domain, to virus persistence by maintaining a low level of HCV replication.

Materials and methods

Plasmid construction

pT7ΔloopILuc (termed ΔILuc in this report), a 271-nt fragment containing a T7 promoter followed by nt 23–249 from the 5' terminus of the HCV genome (clone NIHJ1; genotype 1b) (Aizaki et al., 1998), was amplified by PCR using pT7HCVLuc (HCVLuc) (Shimoike et al., 1999) as a template and primers HindIIIT7S (5'-CCCAAGCTTTAATACGACT-CACTATACACTCCACCATAG-3') and NheIAS (5'-CTAGC-TAGCAGTCTCGCGCGGGG-3'). The PCR product was digested with both HindIII and NheI and ligated with a 5.3-kbp HindIII–NheI fragment of pT7HCVLuc. pT7Δ23–41Luc (Δ23–41Luc) was made using a QuickChange Site-Directed Mutagenesis Kit (Stratagene, La Jolla, CA) in order to introduce a deletion of nt 23–41 from the 5' terminus. The primers used for PCR were 23–41S (5'-CCTAGATTGGGGGCGACCCCT-GTGAGGAAC-3') and the 23–41 AS complement (5'-GTTCCTCACAGGGGTCGCCCCCAATCAGG-3'), and pT7HCVLuc was used as a template.

pT7ΔIIIdLuc (ΔIIIdLuc) was made by digestion of pT7HCVLuc with NheI and StuI, thereby generating 30-bp (corresponding to the stem-loop IIId region), 1.8-kbp, and 3.8-kbp fragments. After this, the 1.8-kbp and 3.8-kbp fragments were isolated, blunt-ended, and then ligated.

pT72a2bLuc (2a2bLuc), pT7BVDVLuc (BVDVLuc), pT7IIId-1Luc (IIId-1Luc), and pT7IIId-2Luc (IIId-2Luc) were

made as follows. pT7HCVLuc was partially digested with StuI. A 5.6-kbp fragment was isolated and completely digested with NheI. The resulting fragment was ligated with annealed two partially complementary oligonucleotides with the following NheI and StuI sites: 5'-CTAGCCGAGTAGTGTTGGGTCGCGACTAGG-3' and 5'-CCTAGTCGCGACCCAACACTACTCGG-3' for IIId-1,5'-CTAGCCGAGTAGTGTTCCCTCGCGAAAGG-3' and 5'-CCTTTCGCGAGGGAACACTACTCGG-3' for IIId-2, 5'-CTAGCCGAGTAGCGTTGGGTTGCGAAAGG-3' and 5'-CCTTTCGCAACCCAACGCTACTCGG-3' for 2a2b, and 5'-CTAGCCTGAGCGGGGGTCGCCCAGG-3' and 5'-CCTG-GGCGACCCCCGCTCAGG-3' for BVDVLuc (the underlined nucleotides were substituted for the wild type nucleotides; see Fig. 4A).

pRLucHCVLuc, pRLucΔ23–41Luc, and pRLucΔIIIdLuc: 2.6-kb fragments were amplified by PCR using pT7HCVLuc, pT7Δ23–41Luc, and pT7ΔIIIdLuc as template DNAs, respectively, and primers XbaI 5'endS (5'-GCTCTAGAGCCAGC-CCCCGATTGGGGGCGA) and XbaI 3'endAS (5'-GCTC-TAGAACTAGTGGATCCGGAT). The PCR products were digested with XbaI and ligated with a 3.3-kb XbaI fragment of pRL-null Vector (Promega, Madison, WI).

pRLucΔILuc: 2.6-kb fragment was amplified by PCR using pT7ΔILuc as a template DNA and primers XbaIloopIS (5'-GCTCTAGACACTCCACCATAGATCACCCCC) and XbaI 3'endAS. The PCR product was digested with XbaI and ligated with a 3.3-kb XbaI fragment of pRL-null Vector.

pCAGC191 (Suzuki et al. 2001) carries nt 329–914, containing the entire HCV coding region of the core protein of clone HCV J1 (Aizaki et al. 1998), controlled by the CAG promoter. pCAGFS contains a frame shift mutation, involving substitution of A with T at nt 357, to make a stop codon (TAA)

(refer to Fig. 1). Only the first five residues (MSTNP) of the core protein are translated from this plasmid. To create a series of mutated core-expressing constructs: pCAGC191m1, -m2, -m3, -m4, -m5, -m6, and -m7, alanine substitutions were introduced into the basic-residue clusters of the core protein by PCR mutagenesis with primers containing base alterations, as described previously (Suzuki et al., 2005). The PCR products were then cloned into pCR2.1 (Invitrogen Corp., Carlsbad, CA) and verified by DNA sequencing. Individual cDNAs were excised and inserted separately into pCAGGS. The primer sequences used in these constructions are available from the authors upon request.

Cells

A human hepatocellular carcinoma cell line, HepG2, was obtained from the American Type Culture Collection. Cells were maintained in Dulbecco's modified Eagle's medium (Nissui, Tokyo, Japan) containing 50 µg/ml of Gentamycin (Biological Industries Ltd., Israel) and supplemented with 10% fetal calf serum.

RNA preparation

The reporter plasmids were linearized by digestion with adequate restriction enzymes, and the resulting DNA fragments were used as templates for in vitro transcription. HCVLuc and a series of HCVLuc mutants were linearized by digestion with XhoI. pRL-null (Promega, Madison WI) was linearized by XbaI digestion. pRLucHCVLuc and a series of pRLucHCVLuc mutants were linearized by BamHI digestion. An in vitro transcription kit, MEGAscript (Ambion, Austin, TX), was used for RNA synthesis, during which reaction mixtures containing 1 µg of DNA template and 2 µl of T7 enzyme mix were incubated at 37 °C for 2 h. For capped RNA synthesis, linearized pRL-null, pRLucHCVLuc, and a series of pRLucHCVLuc mutants were used as templates, and 2 µl of each ATP, CTP, and UTP (7.5 mM), as well as 1 µl of GTP (7.5 mM) and 1 µl of cap homologue m7G (5') ppp (5') G (7.5 mM; Ambion), was used. The reaction mixtures were subsequently treated twice with 2 U of DNase I at 37 °C for 20 min followed by EDTA (25 mM) and lithium chloride (3.75 M) to terminate the reaction. Capped mRNA synthesized contained 11 nucleotides at 5'UTR and no poly(A) tail.

Transfection

For DNA transfection, 100 µl of Opti-MEM (Invitrogen Corp.) and 4 µl of TransIT-LT1 reagent (Mirus Corp., WI) were mixed and incubated at room temperature for 5 min followed by the addition of 2 µg of each plasmid expressing core protein, mutant core protein, or empty vector followed by incubation for a further 15 min. For RNA transfection, synthesized reporter RNA and 2.5 µl of Tfx-20 (Promega) were mixed in 100 µl of Opti-MEM and incubated for 15 min prior to transfection. One day prior to DNA transfection, cells (2.5×10^5) were seeded into a 12-well plate. The transfection mixture described above was added to the cells in 500 µl of Opti-MEM medium after the cells were washed twice with 500 µl of Opti-MEM.

Luciferase assay

The cells infected or transfected with a recombinant baculovirus or plasmid carrying the entire HCV core gene (AcCA39 or pCAGC191) or an empty vector (AcCAG or pCAGGS) were cultured for 2 days followed by transfection with reporter RNA, either HCVLuc (0.1 µg/well), ΔILuc (6.0 µg/well), Δ23–41Luc (0.2 µg/well), ΔIIIdLuc (6.0 µg/well), IIId-1 (0.1 µg/well), IIId-2 (6.0 µg/well), 2a2bLuc (0.1 µg/well), or BVDVLuc (0.1 µg/well), along with capped RL RNA (0.08 µg/well). After 6 h of incubation, FL and RL activities were determined using the Dual-Luciferase Reporter Assay System (Promega), as previously described (Aoki et al., 1998; Shimoike et al., 1999). Luminescent signals were measured with a TR717 luminometer (Applied Biosystems Japan Ltd., Tokyo, Japan).

Western blot analysis

Expression of HCV core protein was detected by Western blotting, as previously described (Shimoike et al., 1999). Briefly, protein was transferred to a polyvinylidene difluoride (PVDF) membrane (Immobilon; Millipore, Tokyo, Japan) after separation by SDS-PAGE. After blocking, the membranes were probed with a polyclonal antibody against glutathione-S-transferase core (aa 1–191) fusion protein, at a 1:100 dilution.

SPR experimental procedure

To prepare the core protein, insect Tn5 cells were infected with a recombinant baculovirus Ac39. The core protein was partially purified from the cell lysate, as previously described (Tanaka et al., 2000). Interactions between the core protein and synthetic RNA oligonucleotides were examined by SPR analyses with BIAcore 2000 (Biacore K.K., Tokyo, Japan). The SPR experimental procedure was as previously described (Tanaka et al., 2000). Briefly, a biotinylated oligonucleotide spanning nt 251–282 (IIId-wt) and mutant IIId domains (IIId-1 and IIId-2) (Fig. 4A) were synthesized followed by immobilization on streptavidin pre-coated sensor chips. Forty microliters of solution containing the core protein (4 µg/ml) was injected onto the sensor chip surface at a flow rate of 8 µl/min. The sample flow was stopped, and buffer washout started at 5 min post-injection.

Acknowledgments

References

Aizaki, H., Aoki, Y., Harada, T., Ishii, K., Suzuki, T., Nagamori, S., Toda, G., Matsuura, Y., Miyamura, T., 1998. Full-length complementary DNA of hepatitis C virus genome from an infectious blood sample. Hepatology 27, 621–627.

Ali, N., Siddiqui, A., 1995. Interaction of polypyrimidine tract-binding protein with the 5′ noncoding region of the hepatitis C virus RNA genome and its functional requirement in internal initiation of translation. J. Virol. 69, 6367–6375.

Ali, N., Siddiqui, A., 1997. The La antigen binds 5′ noncoding region of the hepatitis C virus RNA in the context of the initiator AUG codon and stimulates internal ribosome entry site-mediated translation. Proc. Natl. Acad. Sci. U.S.A. 94, 2249–2254.

Ali, N., Pruijn, G.J., Kenan, D.J., Keene, J.D., Siddiqui, A., 2000. Human La antigen is required for the hepatitis C virus internal ribosome entry site-mediated translation. J. Biol. Chem. 275, 27531–27540.

Alter, H.J., Seeff, L.B., 2000. Recovery, persistence, and sequelae in hepatitis C virus infection: a perspective on long-term outcome. Semin. Liver Dis. 20, 17–35.

Aoki, Y., Aizaki, H., Shimoike, T., Tani, H., Ishii, K., Saito, I., Matsuura, Y., Miyamura, T., 1998. A human liver cell line exhibits efficient translation of HCV RNAs produced by a recombinant adenovirus expressing T7 RNA polymerase. Virology 250, 140–150.

Anwar, A., Ali, N., Tanveer, R., Siddiqui, A., 2000. Demonstration of functional requirement of polypyrimidine tract-binding protein by SELEX RNA during hepatitis C virus internal ribosome entry site-mediated translation initiation. J. Biol. Chem. 275, 34231–34235.

Boni, S., Lavergne, J.P., Boulant, S., Cahour, A., 2005. Hepatitis C virus core protein acts as a *trans*-modulating factor on internal translation initiation of the viral RNA. J. Biol. Chem. 280, 17737–17748.

Brown, E.A., Zhang, H., Ping, L.H., Lemon, S.M., 1992. Secondary structure of the 5′ nontranslated regions of hepatitis C virus and pestivirus genomic RNAs. Nucleic Acids Res. 20, 5041–5045.

Buratti, E., Tisminetzky, S., Zotti, M., Baralle, F.E., 1998. Functional analysis of the interaction between HCV 5′UTR and putative subunits of eukaryotic translation initiation factor eIF3. Nucleic Acids Res. 26, 3179–3187.

Choo, Q.-L., Richman, K.H., Han, J.H., Berger, K., Lee, C., Dong, C., Gallegos, C., Coit, D., Medina-Selby, A., Barr, P.J., Weiner, A.J., Bradley, D.W., Kuo, G., Houghton, M., 1991. Genetic organization and diversity of the hepatitis C virus. Proc. Natl. Acad. Sci. U.S.A. 88, 2451–2455.

Collier, A.J., Tang, S., Elliott, R.M., 1998. Translation efficiencies of the 5′ untranslated region from representatives of the six major genotypes of hepatitis C virus using a novel bicistronic reporter assay system. J. Gen. Virol. 79, 2359–2366.

Fan, Z., Yang, Q.R., Twu, J.S., Sherker, A.H., 1999. Specific in vitro association between the hepatitis C viral genome and core protein. J. Med. Virol. 59, 131–134.

Friebe, P., Lohmann, V., Krieger, N., Bartenschlager, R., 2001. Sequences in the 5′ nontranslated region of hepatitis C virus required for RNA replication. J. Virol. 75, 12047–12057.

Fukushi, S., Katayama, K., Kurihara, C., Ishiyama, N., Hoshino, F.B., Ando, T., Oya, A., 1994. Complete 5′ noncoding region is necessary for the efficient internal initiation of hepatitis C virus RNA. Biochem. Biophys. Res. Commun. 199, 425–432.

Fukushi, S., Okada, M., Kageyama, T., Hoshino, F.B., Nagai, K., Katayama, K., 2001. Interaction of poly(rC)-binding protein 2 with the 5′-terminal stem loop of the hepatitis C-virus genome. Virus Res. 73, 67–79.

Grakoui, A., McCourt, D.W., Wychowski, C., Feinstone, S.M., Rice, C.M., 1993. Characterization of the hepatitis C virus-encoded serine proteinase: determination of proteinase-dependent polyprotein cleavage sites. J. Virol. 67, 2832–2843.

Hahm, B., Kim, Y.K., Kim, J.H., Kim, T.Y., Jang, S.K., 1998. Heterogeneous nuclear ribonucleoprotein L interacts with the 3′ border of the internal ribosomal entry site of hepatitis C virus. J. Virol. 72, 8782–8788.

Hellen, C.U., Pestova, T.V., 1999. Translation of hepatitis C virus RNA. J. Viral Hepatitis 6, 79–87.

Hijikata, M., Kato, N., Ootsuyama, Y., Nakagawa, M., Shimotohno, K., 1991. Gene mapping of the putative structural region of the hepatitis C virus genome by in vitro processing analysis. Proc. Natl. Acad. Sci. U.S.A. 88, 5547–5551.

Honda, M., Ping, L.H., Rijnbrand, R.C., Amphlett, E., Clarke, B., Rowlands, D., Lemon, S.M., 1996. Structural requirements for initiation of translation by internal ribosome entry within genome-length hepatitis C virus RNA. Virology 222, 31–42.

Honda, M., Beard, M.R., Ping, L.H., Lemon, S.M., 1999a. A phylogenetically conserved stem-loop structure at the 5′ border of the internal ribosome entry site of hepatitis C virus is required for cap-independent viral translation. J. Virol. 73, 1165–1174.

Honda, M., Rijnbrand, R., Abell, G., Kim, D., Lemon, S.M., 1999b. Natural variation in translational activities of the 5′ nontranslated RNAs of hepatitis C virus genotypes 1a and 1b: evidence for a long-range RNA–RNA interaction outside of the internal ribosomal entry site. J. Virol. 73, 4941–4951.

Hwang, S.B., Lo, S.Y., Ou, J.H., Lai, M.M., 1995. Detection of cellular proteins and viral core protein interacting with the 5′ untranslated region of hepatitis C virus RNA. J. Biomed. Sci. 2, 227–236.

Isoyama, T., Kamoshita, N., Yasui, K., Iwai, A., Shiroki, K., Toyoda, H., Yamada, A., Takasaki, Y., Nomoto, A., 1999. Lower concentration of La protein required for internal ribosome entry on hepatitis C virus RNA than on poliovirus RNA. J. Gen. Virol. 80, 2319–2327.

Jubin, R., Vantuno, N.E., Kieft, J.S., Murray, M.G., Doudna, J.A., Lau, J.Y., Baroudy, B.M., 2000. Hepatitis C virus internal ribosome entry site (IRES) stem loop IIId contains a phylogenetically conserved GGG triplet essential for translation and IRES folding. J. Virol. 74, 10430–10437.

Kamoshita, N., Tsukiyama-Kohara, K., Kohara, M., Nomoto, A., 1997. Genetic analysis of internal ribosomal entry site on hepatitis C virus RNA: implication for involvement of the highly ordered structure and cell type-specific transacting factors. Virology 233, 9–18.

Kieft, J.S., Zhou, K., Jubin, R., Murray, M.G., Lau, J.Y., Doudna, J.A., 1999. The hepatitis C virus internal ribosome entry site adopts an ion-dependent tertiary fold. J. Mol. Biol. 292, 513–529.

Kieft, J.S., Zhou, K., Jubin, R., Doudna, J.A., 2001. Mechanism of ribosome recruitment by hepatitis C IRES RNA. RNA 7, 194–206.

Kim, Y.K., Lee, S.H., Kim, C.S., Seol, S.K., Jang, S.K., 2003. Long-range RNA–RNA interaction between the 5′ nontranslated region and the core-coding sequences of hepatitis C virus modulates the IRES-dependent translation. RNA 9, 599–606.

Kolupaeva, V.G., Pestova, T.V., Hellen, C.U., 2000. An enzymatic footprinting analysis of the interaction of 40S ribosomal subunits with the internal ribosomal entry site of hepatitis C virus. J. Virol. 74, 6242–6250.

Li, D., Takyar, S.T., Lott, W.B., Gowans, E.J., 2003. Amino acids 1–20 of the hepatitis C virus (HCV) core protein specifically inhibit HCV IRES-dependent translation in HepG2 cells, and inhibit both HCV IRES- and cap-dependent translation in HuH7 and CV-1 cells. J. Gen. Virol. 84, 815–825.

Lo, S.-Y., Selby, M.J., Ou, J.-H., 1996. Interaction between hepatitis C virus core protein and E1 envelope protein. J. Virol. 70, 5177–5182.

Lu, H.H., Wimmer, E., 1996. Poliovirus chimeras replicating under the translational control of genetic elements of hepatitis C virus reveal unusual

properties of the internal ribosomal entry site of hepatitis C virus. Proc. Natl. Acad. Sci. U.S.A. 93, 1412–1417.

Lukavsky, P.J., Otto, G.A., Lancaster, A.M., Sarnow, P., Puglisi, J.D., 2000. Structures of two RNA domains essential for hepatitis C virus internal ribosome entry site function. Nat. Struct. Biol. 7, 1105–1110.

Luo, G., Xin, S., Cai, Z., 2003. Role of the 5′-proximal stem-loop structure of the 5′ untranslated region in replication and translation of hepatitis C virus RNA. J. Virol. 77, 3312–3318.

Moriishi, K., Okabayashi, T., Nakai, K., Moriya, K., Koike, K., Murata, S., Chiba, T., Tanaka, K., Suzuki, R., Suzuki, T., Miyamura, T., Matsuura, Y., 2003. Proteasome activator PA28gamma-dependent nuclear retention and degradation of hepatitis C virus core protein. J. Virol. 77, 10237–10249.

Odreman-Macchioli, F.E., Tisminetzky, S.G., Zotti, M., Baralle, F.E., Buratti, E., 2000. Influence of correct secondary and tertiary RNA folding on the binding of cellular factors to the HCV IRES. Nucleic Acids Res. 28, 875–885.

Otto, G.A., Lukavsky, P.J., Lancaster, A.M., Sarnow, P., Puglisi, J.D., 2002. Ribosomal proteins mediate the hepatitis C virus IRES–HeLa 40S interaction. RNA 8, 913–923.

Pawlotsky, J.M., 2004. Pathophysiology of hepatitis C virus infection and related liver disease. Trends Microbiol. 12, 96–102.

Reynolds, J.E., Kaminski, A., Kettinen, H.J., Grace, K., Clarke, B.E., Carroll, A.R., Rowlands, D.J., Jackson, R.J., 1995. Unique features of internal initiation of hepatitis C virus RNA translation. EMBO J. 14, 6010–6020.

Rijnbrand, R.C.A., Lemon, S.M., 1999. Internal ribosomal entry site-mediated translation in hepatitis C virus replication. In: Hagedorn, C.H., Rice, C.M. (Eds.), The Hepatitis C Viruses. Springer-Verlag, Berlin, Germany, pp. 85–116.

Rijnbrand, R., Bredenbeek, P., van der Straaten, T., Whetter, L., Inchauspe, G., Lemon, S., Spaan, W., 1995. Almost the entire 5′ non-translated region of hepatitis C virus is required for cap-independent translation. FEBS Lett. 365, 115–119.

Santolini, E., Migliaccio, G., La Monica, N., 1994. Biosynthesis and biochemical properties of the hepatitis C virus core protein. J. Virol. 68, 3631–3641

Shimoike, T., Mimori, S., Tani, H., Matsuura, Y., Miyamura, T., 1999. Interaction of hepatitis C virus core protein with viral sense RNA and suppression of its translation. J. Virol. 73, 9718–9725.

Sizova, D.V., Kolupaeva, V.G., Pestova, T.V., Shatsky, I.N., Hellen, C.U., 1998.

Specific interaction of eukaryotic translation initiation factor 3 with the 5′ nontranslated regions of hepatitis C virus and classical swine fever virus RNAs. J. Virol. 72, 4775–4782.

Spahn, C.M., Kieft, J.S., Grassucci, R.A., Penczek, P.A., Zhou, K., Doudna, J.A., Frank, J., 2001. Hepatitis C virus IRES RNA-induced changes in the conformation of the 40s ribosomal subunit. Science 291, 1959–1962.

Spangberg, K., Schwartz, S., 1999. Poly(C)-binding protein interacts with the hepatitis C virus 5′ untranslated region. J. Gen. Virol. 80, 1371–1376.

Suzuki, R., Tamura, K., Li, J., Ishii, K., Matsuura, Y., Miyamura, T., Suzuki, T., 2001. Ubiquitin-mediated degradation of hepatitis C virus core protein is regulated by processing at its carboxyl terminus. Virology 280, 301–309.

Suzuki, R., Sakamoto, S., Tsutsumi, T., Rikimaru, A., Tanaka, K., Shimoike, T., Moriishi, K., Iwasaki, T., Mizumoto, K., Matsuura, Y., Miyamura, T., Suzuki, T., 2005. Molecular determinants for subcellular localization of hepatitis C virus core protein. J. Virol. 79, 1271–1281.

Takamizawa, A., Mori, C., Fuke, I., Manabe, S., Murakami, S., Fujita, J., Onishi, E., Andoh, T., Yoshida, I., Okayama, H., 1991. Structure and organization of the hepatitis C virus genome isolated from human carriers. J. Virol. 65, 1105–1113.

Tallet-Lopez, B., Aldaz-Carroll, L., Chabas, S., Dausse, E., Staedel, C., Toulme, J.J., 2003. Antisense oligonucleotides targeted to the domain IIId of the hepatitis C virus IRES compete with 40S ribosomal subunit binding and prevent in vitro translation. Nucleic Acids Res. 31, 734–742.

Tanaka, Y., Shimoike, T., Ishii, K., Suzuki, R., Suzuki, T., Ushijima, H., Matsuura, Y., Miyamura, T., 2000. Selective binding of hepatitis C virus core protein to synthetic oligonucleotides corresponding to the 5′ untranslated region of the viral genome. Virology 270, 229–236.

Tsukiyama-Kohara, K., Iizuka, N., Kohara, M., Nomoto, A., 1992. Internal ribosome entry site within hepatitis C virus RNA. J. Virol. 66, 1476–1483.

Wang, T.H., Rijnbrand, R.C., Lemon, S.M., 2000. Core protein-coding sequence, but not core protein, modulates the efficiency of cap-independent translation directed by the internal ribosome entry site of hepatitis C virus. J. Virol. 74, 11347–11358.

Zhang, J., Yamada, O., Yoshida, H., Iwai, T., Araki, H., 2002. Autogenous translational inhibition of core protein: implication for switch from translation to RNA replication in hepatitis C virus. Virology 293, 141–150.

Zhao, W.D., Wimmer, E., 2001 Genetic analysis of a poliovirus/hepatitis C virus chimera: new structure for domain II of the internal ribosomal entry site of hepatitis C virus. J. Virol. 75, 3719–3730.

BASIC RESEARCH

Reconstruction of liver organoid using a bioreactor

Masaya Saito, Tomokazu Matsuura, Takahiro Masaki, Haruka Maehashi, Keiko Shimizu, Yoshiaki Hataba, Tohru Iwahori, Tetsuro Suzuki, Filip Braet

Masaya Saito, Division of Gastroenterology and Hepatology, Department of Internal Medicine, The Jikei University School of Medicine, Tokyo, Japan
Tomokazu Matsuura, Department of Laboratory Medicine, The Jikei University School of Medicine, Tokyo, Japan
Takahiro Masaki, Tetsuro Suzuki, Department of Virology II, National Institute of Infectious Disease, Tokyo, Japan
Haruka Maehashi, Keiko Shimizu, First Department of Biochemistry, The Jikei University School of Medicine, Tokyo, Japan
Yoshiaki Hataba, DNA Medical Institute, The Jikei University School of Medicine, Tokyo, Japan
Tohru Iwahori, Fifth Division of Blood Purification, Department of Surgery, Tokyo Medical University, Tokyo, Japan
Filip Braet, Australian Key Center for Microscopy & Microanalysis, Electron Microscope Unit, The University of Sydney, NSW 2006, Australia
Correspondence to: Tomokazu Matsuura, MD, PhD, Department of Laboratory Medicine, The Jikei University School of Medicine, 3-25-8 Nishi-shinbashi, Minato-ku,
Tokyo 105-8461, Japan. matsuurat@jikei.ac.jp
Telephone: +81-3-34331111-3210 Fax: +81-3-34350569

Abstract

AIM: To develop the effective technology for reconstruction of a liver organ *in vitro* using a bio-artificial liver.

METHODS: We previously reported that a radial-flow bioreactor (RFB) could provide a three-dimensional high-density culture system. We presently reconstructed the liver organoid using a functional human hepatocellular carcinoma cell line (FLC-5) as hepatocytes together with mouse immortalized sinusoidal endothelial cell (SEC) line M1 and mouse immortalized hepatic stellate cell (HSC) line A7 as non parenchymal cells in the RFB. Two x 10^7 FLC-5 cells were incubated in the RFB. After 5 d, 2 x 10^7 A7 cells were added in a similar manner followed by another addition of 10^7 M1 cells 5 d later. After three days of perfusion, some cellulose beads with the adherent cells were harvested. The last incubation period included perfusion with 200 nmol/L swinholide A for 2 h and then the remaining cellulose beads along with adherent cells were harvested from the RFB. The cell morphology was observed by transmission electron microscopy (TEM) and scanning electron microscopy (SEM). To assess hepato-

cyte function, we compared mRNA expression for urea cycle enzymes as well as albumin synthesis by FLC-5 in monolayer cultures compared to those of single-type cultures and cocultures in the RFB.

RESULTS: By transmission electron microscopy, FLC-5, M1, and A7 were arranged in relation to the perfusion side in a liver-like organization. Structures resembling bile canaliculi were seen between FCL-5 cells. Scanning electron microscopy demonstrated fenestrae on SEC surfaces. The number of vesiculo-vacuolar organelles (VVO) and fenestrae increased when we introduced the actin-binding agent swinholide-A in the RFB for 2h. With respect to liver function, urea was found in the medium, and expression of mRNAs encoding arginosuccinate synthetase and arginase increased when the three cell types were cocultured in the RFB. However, albumin synthesis decreased.

CONCLUSION: Co-culture in the RFB system can dramatically change the structure and function of all cell types, including the functional characteristics of hepatocytes. Our system proves effective for reconstruction of a liver organoid using a bio-artificial liver.
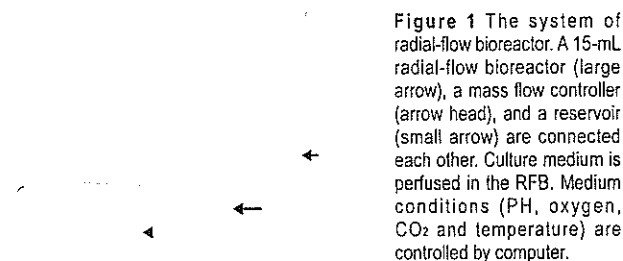
INTRODUCTION

Liver regeneration technology has made many advances in recent years. Efforts now are being made toward development of embryonic stem cells (ES cells), differentiation of hemopoietic stem cells, and development of isolation and culture methods for somatic stem cells originating from different organs. Hemopoietic stem cells, hepatoblasts originating from fetal liver, hepatocytes, and pancreatic duct epithelial cells have been included in the list of candi-

date cells for liver regeneration[1]. Development of immortalized cells by introduction of the simian virus 40 (SV40) large T antigen gene or human telomerase reverse transcriptase (hTERT) is also under investigation[2]. To date, however, no technique for regenerating and reconstructing parenchymal organs using these cells has been established. Conventional cell culture methods have achieved this goal clinically for skin, cornea, and bone tissue[3-5].

Reconstruction of organs such as the liver requires maintenance of viable cells at a high density and coculture under conditions favorable to several different cell types that constitute a liver. To make a culture system is important in reconstructing a liver organoid. Conventional stationary culture techniques are not well suited to the culture of cells in a layered form, i.e., in a structural and functional organoid a simple air/CO₂ incubator does not deliver adequate oxygen supply to layered cells. Furthermore, high-density culture cannot be maintained with the limited nutrients available in conventional cultures. For these reasons, construction of a bioreactor that allows 3-dimensional growth in a high-density perfusion culture has been advocated for reconstructing a liver organoid. In our study a radial-flow bioreactor (RFB) developed in Japan was used as a candidate model for high-density perfusion culture. Filled with a porous carrier, this bioreactor permits culture at a cell density 10 times higher than that allowed by a hollow-fiber culture system[6, 7]. Another important point is to select a cell source. Clinically, cells using bio-artificial liver are required to be highly functional and supplied quickly in large quantities. Therefore we established a functional human hepatocellular carcinoma cell line (FLC-5), which can express drug-metabolized enzymes (e.g., human-type carboxyl esterase or cytochrome) and liver-specific proteins such as albumin. In vitro this cell line retains its three-dimensional form, developing distinct microvilli on the surface. These cells can be cultured in serum-free ASF104 medium (Ajinomoto, Tokyo). A liver organoid cannot be reconstructed with hepatocytes only. At minimum, coculture of hepatocytes with nonparenchymal cells, such as sinusoidal endothelial cell (SEC) and hepatic stellate cell (HSC) is required. So we established immortalized SEC line M1[8] and an immortalized HSC line A7[9] by isolating nonparenchymal cells from an H-2Kb-tsA58-transgenic mouse liver transfected with the SV40 large T antigen gene[10].

Reconstruction of the liver sinusoid is important for activity of the liver organoid as a functional unit. Also, the open pores on the surfaces of SEC in fenestrae have an important functional role in the liver sinusoid. Fenestrae are the most remarkable characteristics of SEC, as first described by Wisse in 1970[11] using transmission electron microscopy (TEM). Diameters of these pores vary between species, ranging from 100 to 200 nm[12]. These fenestrae facilitate the transport of materials and solutes from the luminal to the abluminal side of the liver parenchymal cells and vice versa[13]. The process and mechanism of formation of these pores remain largely unclarified[14, 15]. The presence of actin filaments at the margin of these pores has been demonstrated by electron microscopic studies[16, 17]. Swinholide A, a most potent microfilament-disrupting drug available, has been demonstrated to increase the number

of SEC fenestrae[14]. However, when immortalized SEC was treated in a monolayer culture or as a monoculture in the RFB, an increase in number of fenestrae could not be observed when the Swinholide A was introduced. The potential for drug-induced increase also has been reported to disappear in long-term cultures[8].

In developing a high functioning organoid using a bio-artificial liver, the function, form and reactivity of pharmacological agent should be near in vivo. In the present study, we reconstructed a functional liver organoid using immortalized cell lines in the RFB.

MATERIALS AND METHODS

Cell culture and medium

We used the three cell lines mentioned above, FLC-5, M1, and A7. As reported, culture of M1 cells was possible in serum-free conditions while supplementation of ASF104 medium with 2% fetal bovine serum (FBS) was required for culture of A7 cells. Therefore, in coculture experiments, ASF104 medium was enriched with 2% FBS.

Coculture in radial-flow bioreactor

As reported elsewhere, the RFB system is composed of a 15-mL radial-flow chamber (RA-15; ABLE, Tokyo), a mass flow controller (RAD925, ABLE), a reservoir (Figure 1), a computer, and a tissue incubator as described previously[18] (Figure 1). The culture medium was oxygenated within the reservoir, and the pH was adjusted automatically to 7.4. Oxygen pressure in the culture medium was measured both within the reservoir and at the outlet of the bioreactor. Relative oxygen consumption was monitored on the basis of the oxygen pressure gradient. During the study the temperature within the reservoir was kept constantly at 37 °C. Two × 10⁷ FLC-5 cells were inoculated into the reservoir. The bioreactor was perfused in a closed circuit for 2 h to aid cells in adhering to the porous carrier cellulose beads (Asahi Kasei, Tokyo). Subsequently the bioreactor was switched to the open-circuit mode, and incubation was continued with addition of fresh culture medium to the reservoir. After 5 d, 2 × 10⁷ A7 cells were added in a similar manner followed by another addition of 10⁷ M1 cells 5 d later. Retinol (10⁻⁶mol/L) was added during the first 2 d. After three days of perfusion cellulose beads with the adherent cells were harvested, and cells deposited at the bottom of the bioreactor also were recovered. Beads with attached cells were fixed in 1.2% or 2.0% glutaraldehyde as described below.

Swinholide A experiments

We cultured the three cell lines as described above. The

Figure 1 The system of radial-flow bioreactor. A 15-mL radial-flow bioreactor (large arrow), a mass flow controller (arrow head), and a reservoir (small arrow) are connected each other. Culture medium is perfused in the RFB. Medium conditions (PH, oxygen, CO₂ and temperature) are controlled by computer.

last incubation included perfusion with 200 nmol/L swinholide A (Sigma catalog number S9810; S) for 2 h. The cellulose beads along with adherent cells were harvested from the bioreactor. Beads with attached cells were fixed in glutaraldehyde and prepared for morphologic observation as follows.

Electron microscopy

For scanning electron microscopy (SEM), cultured cells were fixed with 1.2% glutaraldehyde in 0.1 mol/L phosphate buffer (PB) at pH 7.4 and postfixed with 1% OsO_4 in 0.1mol/L PB. The fixed cells were rinsed twice with PBS, subsequently dehydrated in ascending concentrations of ethanol, critical point-dried using carbon dioxide, and coated by vacuum- evaporated carbon and ion-spattered gold. Specimens were observed under JSM-35 scanning electron microscope (JEOL, Tokyo) at an accelerated voltage of 10 kV.

For transmission electron microscopy (TEM), cultured cells were fixed with 2.0% glutaraldehyde in 0.1mol/L PB for 1 h and postfixed with 1% OsO_4 in 0.1mol/L PB for 1 h at 4 ℃. Specimens were dehydrated in ethanol and subsequently embedded in a mixture of Epon-Araldite. Thin sections (60 nm) were cut with a diamond knife mounted on an LKB ultratome, and stained with aqueous uranyl acetate. Specimens were examined under a JEOL 1200EX electron microscope.

Amino acid analysis of supernatants

For analysis of amino acid fractions by high-performance liquid chromatography (HPLC), supernatants were collected from FLC-5 alone and from cocultures of the three cell types in the bioreactor. Supernatants were mixed with 5% sulfosalicylic acid and allowed to stand at 4 ℃ for 15 min. After centrifugation to precipitate protein, supernatants were injected into amino acid analysis columns (L-8500, Hitachi, Tokyo).

Quantitative TaqMan RT-PCR

We measured mRNA expression for the urea cycle enzymes, carbamoyl phosphate synthetase (CPS1), ornithine carbamoyltransferase (OCT), argininosuccinatesynthetase (ASS), argininosuccinatelyase (ASL), and arginase (ARG), as well as mRNA expression for albumin, hepatocyte nuclear factor (HNF)-1 and HNF-4, by quantitative TaqMan reverse transcription polymerase chain reaction (RT-PCR). RT-PCR was performed on the ABI PRISM 7700 sequence detection system using random hexamers from TaqMan reverse transcription reagents and the RT reaction mix (Applied Biosystems, Rockville, M) to reverse-transcribe RNA. TaqMan universal PCR Master Mix and Assays-on-Demand gene expression probes (Applied Biosystems) were used for PCR. A standard curve for serial dilution of 18S rRNAs was generated similarly. A relative standard curve method (Applied Biosystems) was used to calculate the amplification difference in urea cycle-related enzymes between cocultured and control cells, and elongation factor 1 (EF1), for each primer set and between albumin, HNF-1, HNF-4, and glyceraldehyde-3-phosphate dehydrogenase (GAPDH). Specificity was evaluated using GAPDH mRNA as an internal control (4310884E; Perkin-
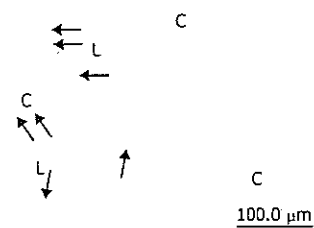

Figure 2 Light microscopic image of coculture in the RFB. High-density and layered cells attached on the cellulose beads (C). Sinusoid-like lumen structure (L) could be observed. SEC was observed with flat shape on surface of the lumen and perfusion side (arrow).

100.0 μm

Elmer Applied Biosystems). Each amplification was performed in triplicate, and averages were obtained.

Based on DNA sequences in GenBank, primers and the TaqMan probe for albumin, HNF-1, and HNF-4 were designed using the primer design software Primer Express TM (Perkin-Elmer Applied Biosystems, Foster City, CA). AmpliTaq DNA polymerase extended the primer and displaced the TaqMan probe through its 5'-3' exonuclease activity. Probes were labeled with a reporter fluorescent dye either 6-carboxy-fluorescein (FAM) or 2, 7 dimethoxy-4,5-dichloro-6-carboxy-fluorescein (JOE) at the 5' end and a quencher fluorescent dye [6-carboxytetramethyl-rhodamine (TAMRA)] at the 3' end.

Primers/probes were as follows: ornithine transcarbamoylase (OTC) forward primer 5'-CCAGGCAATA-AAAGAGTCAGGATT-3', reverse primer/ 5'-TTAT-CAAAG TCCCCTGGTTAGAGATACT-3', probe/ 5'-(FAM)- TTCAAATGCTCCTACACCCTGCCCTG-(TAMRA)-3'; arginosuccinase (ASL) forward primer/ 5'-TGGCCAAGGAGGTCGTCA-3', reverse primer 5'-TTCCTCGTCGTCCGGAAG-3', probe 5'-(FAM)-TGTCTTCCAGACCCGGAGACCGAA-(TAMRA)-3'; albumin forward primer/ 5'-CGATTTTCTTTT-TAGGGCAGTAGC-3', reverse primer/ 5'-TG-GAAACTTCTGCAAACTCAGC-3', probe/ 5'-(FAM)-CGCCTGAGCCAGAGATTTCCCA-(TAMRA)-3'; HNF-1 forward primer/ 5'-AGCGGGAGGTGGTC-GATAC-3', reverse primer/ 5'-CATGGGAGTGCCCTT-GTTG-3', probe/ 5'-(FAM)-TCAACCAGTCCCACCT-GTCCCAACA-(TAMRA)-3'; HNF-4 forward primer/ 5'-GGTGTCCATACGCATCCTTGA-3', reverse primer/ 5'-TGGCTTTGAGGTAGGCATACTCA-3', probe/ 5'-(FAM)-CCTTCCAGGAGCTGCAGATC-GATGAC-(TAMRA)-3'; GAPDH forward primer/ 5'-CTCCCACACACATGCACTTA-3', reverse primer/ 5'-CCTAGTCCCAGGGCTTTGATT-3', probe/ 5'-(VIC)-AAAAGAGCTAGGAAGGACAGGCAACTTGGC-(TAMRA)-3'.

RESULTS

Structure of cells cultured in bioreactor

In the bioreactor, cells cultured in high density assumed layered form on the cellulose beads. Lumen-like structure was observed. Endothelial cells were exits with flat shape at the surface of the lumen and the perfusion side (Figure 2). Multiple layers of FLC-5 cells adhered to the cellulose beads, while A7 and M1 cells were predominantly localized to the side where perfusion occurred. Layered cells were seen in a hole of porous cellulose beads. Sinusoid-like lumen was observed at perfusion side in the cellulose beads
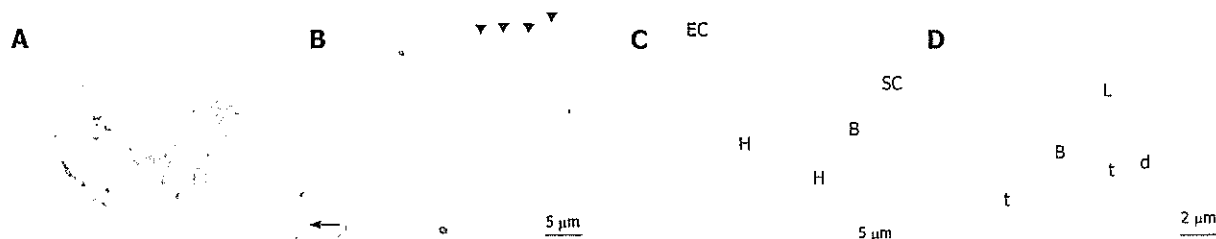
Figure 3 Transmission electron microscopic images of cocultures in the RFB. A: The cells are arrayed on the cellulose beads. Several cell clusters could be seen in a gap of cellulose beads (arrow). Vascular lumen structure surrounding cell clusters could be seen in the beads (small arrow). Culture media flow through inside of lumen structure; B: The cells are arrayed in layers on cellulose beads. Part of a cellulose bead (arrow) is visible at the bottom of the layer. A process of a sinusoidal endothelial cell (arrowhead) is seen at the perfusion side. Scale bar: 5 μm; C: Sinusoidal endothelial cells (EC) can be seen at the perfusion side. Hepatic stellate cells (SC) containing fatty vitamin A droplets are seen overlying the FLC-5 cells (H). FLC-5 cells (H) below EC and SC show bile-canaliculus-like structures (B). Scale bar: 5 μm. D: Bile canaliculus-like structures (B) containing electron dense bile components. Tight junctions (t) and desmosomes (d) are visible, as are fatty vitamin A droplets (L). Scale bar: 2 μm.
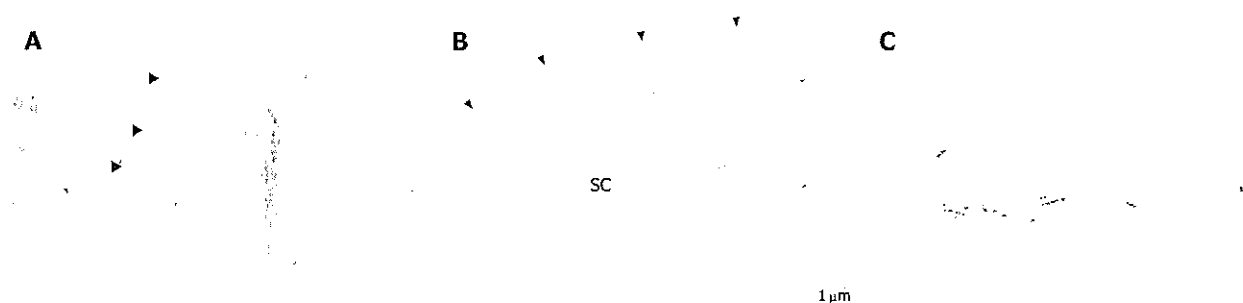
Figure 4 Ultrastructure of sinusoidal endothelial cells. A: Scanning electron microscopic image of sinusoidal endothelial cells localized at the perfusion side. They form a thin layer (arrowhead), showing the typical appearance of a sinusoid-like vascular structure. Scale bar: 5 μm; B: Transmission electron microscopic image showing sinusoidal endothelial cell growth at the perfusion side forming a thin layer (arrowhead) overlying the A7 cells (SC). Scale bar: 1 μm; C: Transmission electron microscopic view showing tight junctions (arrow) between sinusoidal endothelial cells (EC). Scale bar: 200 nm.
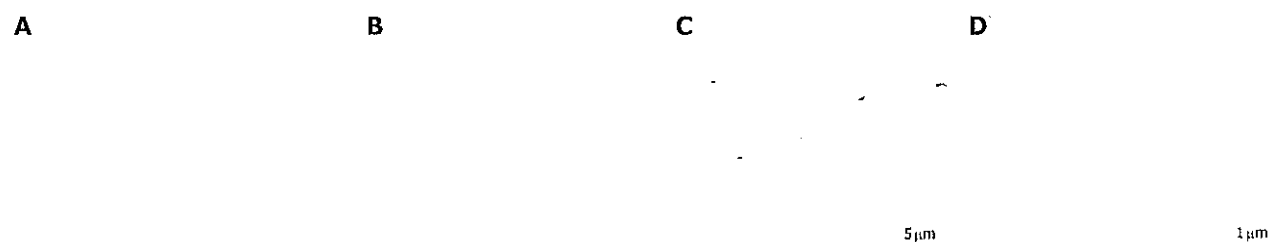

Figure 5 Scanning electron microscopic image of the surface of sinusoidal endothelial cells. A: Low-magnification scanning electron microscopic images of the surface of sinusoidal endothelial cells cultured on plastic dishes. The sinusoidal endothelial cells formed a thin layer on the plastic dish substrate. Scale bar: 5 μm; B: High-magnification scanning electron microscopy images of the surface of sinusoidal endothelial cells cultured on plastic dishes. Fenestrae could not be detected on the surface of endothelial cells. Only small pits are seen (arrow). Scale bar: 1 μm; C: Low-magnification scanning electron microscopic view of the surface of sinusoidal endothelial cells cocultured in the RFB. Fenestrated pores could be observed (arrow). Scale bar: 5 μm; D: High-magnification scanning electron microscopic view of the surface of sinusoidal endothelial cells cocultured in the RFB. Pores have a diameter of 100 - 200 nm. Scale bar: 1 μm.

(Figure 3A). TEM showed that cocultured cells assumed layered form from cellulose beads to the perfusion side (Figure 3B). M1 and A7 cells containing vitamin A-laden fat droplets were seen mainly at the perfusion side, while dense layers of FLC-5 cells were observed beneath (Figure 3C). At sites where the three cell lines were in contact with each other bile canaliculus-like structures were present between neighboring FLC-5 cells. Lumens of these structures contained electron-dense bile components, tight junctions and desmosomes also could be observed (Figure 3D). This side showed growth of endothelial cells with the formation of sinusoid-like vascular structures (Figures 4A and 4B). Tight junctions were seen between endothe-

lial cells (Figure 4C). Fenestrae which are characteristic of SEC *in vivo*, were absent in monocultures of M1 cells on plastic dishes (Figures 5A and 5B). Because a long time subculture would change the character of M1 cells, pores were represent on the surface of M1 cells co-cultured in the RFB system (Figure 5C). The pores had a diameter of 100 to 200 nm, being similar in morphology and size to those of fenestrae shown by SEC *in vivo* (Figure 5D).

*Morphology of M1 cells incubated with swinholide A*
Cells incubated for 2 h with 200 nmol/L of the actin-disrupting agent swinholide A showed the increased number of pores (Figure 6), while some pores were dilated (about

A

1 µm

B.

200 nm   200 nm
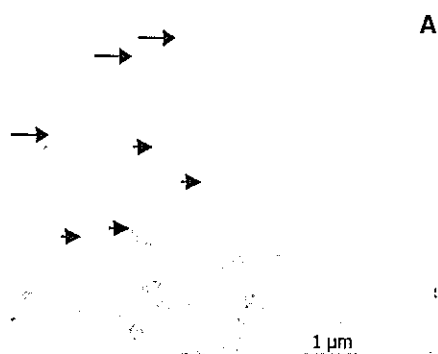
Figure 6 Scanning electron micrographs of the surface of swinholide A - treated SEC cells in the RFB culture system. Large open pores have a fenestra-like appearance (short arrow). Small pores were detectable in the nonfenestrated area (long arrow). Scale bar: 1 µm.
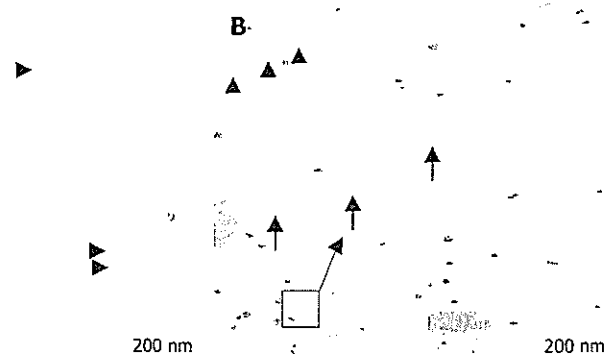
Figure 7 Transmission electron micrographs of sectioned SEC cells after swinholide A - treatment; A: Numerous open pores or fenestrae in the cytoplasm (arrow). Fine cytoskeletal elements showing a close spatial relationship with these pores (arrowhead). Scale bar: 200 nm; B: VVO could be observed in SEC cells (arrows) in response to stress or actin fibers (arrowheads). Scale bar: 200 nm. Inset shows the overall composition of the cells. Scale bar: 1 µm.
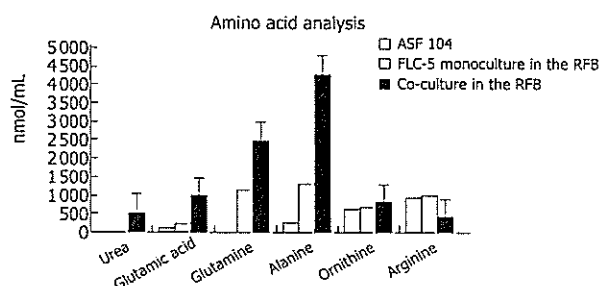
Figure 8 Amino acid and urea analysis in supernatants. Urea was detectable only in coculture, at 523 nmol/ml. ASF 104 designates culture medium. Mean value ± SD.
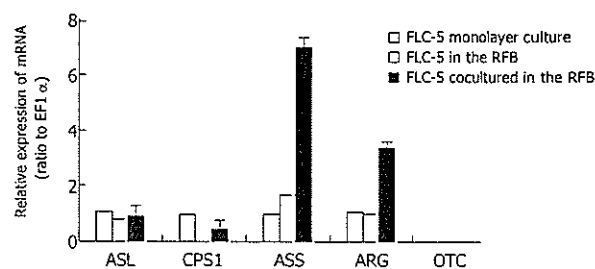

Figure 9 Comparison of expressions of CPS1, OTC, ASS, ASL, and ARG mRNA in FLC-5 incubated under different conditions as assessed by TaqMan 1-step RT-PCR. The mRNA expression of each enzyme in different conditions is relative to that in monolayer cultures. Mean value ± SD.

1 µm). Small pores (tens of nanometers in size) that probably resembled coated pits were abundant in the nonfenestrated areas.

TEM investigation showed that treatment with swinholide A resulted in fenestrated pores with a diameter between 100 and 200 nm. The pores fused with each other formed labyrinthine structures (Figure 7A). In addition, vacuoles with a diameter of about 200 nm, similar to previously described vesiculo vacuolar organelles (VVO), were noted. These structures typically were seen in areas where relatively regular overlap was seen in FLC-5, A7, and M1. The number of VVO increased when cells were treated with 200 nmol/L swinholide A, which was associated with partial fusion (Figure 7B).

Amino acid fractions from supernatants

At the end of culture, the supernatant was subjected to amino acid analysis. Urea production was not seen in monocultures of FLC-5 cells in the RFB, while FLC-5 cells cocultured with M1 and A7 cells produced 523 nmol urea /mL in the culture medium, suggesting that the urea cycle was activated in the coculture RFB system (Figure 8). Several amino acids were increased in the medium.

We compared mRNA expression of CPS1, OTC, ASS, ASL, and ARG in FLC-5 monolayer cultures with those of monocultures in the RFB system. In addition, mRNA expression in cocultures in the RFB also was assessed. We

could not detect OTC in any type of culture. Expression of other urea cycle enzymes showed no notable difference between monolayer culture of FLC-5 and monoculture of FLC-5 in the RFB. However, ASS and ARG expressions in co-culture in the RFB were about 7 and 3 times greater than those in FLC-5 monolayer culture (Figure 9).

Albumin synthesis and expression of nuclear factors

We compared mRNA expression of albumin and HNF-1 and HNF-4 as transcription regulation factors between experimental conditions. Expression of mRNA encoding the three proteins was less in FLC-5 co-cultures in the RFB system than in FLC-5 RFB monocultures or in FLC-5 cells in monolayer culture (Figures 10A-10C). In a previous study, albumin production was enhanced in the RFB using the immortalized cell line[18]. However it was different cell line in this study.

DISCUSSION

Introduction of a functional human hepatocellular carcinoma cell line (FLC) in our system can allow the cells to be cultured at high density in a layered array and maintain viability for long periods[18,19].

Immortalized cells can be used for artificial liver. The reason is that it can supply cells in large quantities and quickly. Immortalized cells lose several characteristics in
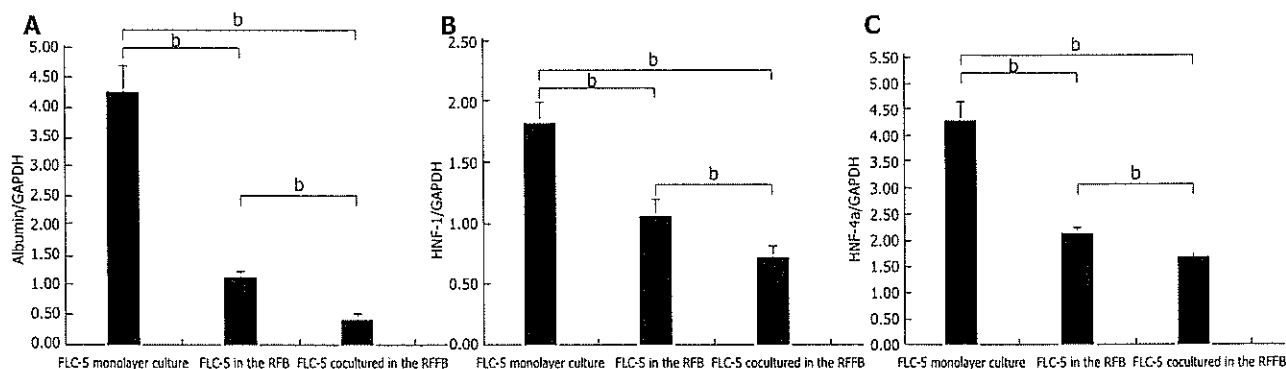
Figure 10 Expression of mRNA for albumin (A), HNF-4 (B) and HNF-1 (C) as transcription regulation factors in each condition. Messenger RNA expression for these three proteins decreased in cocultured FLC-5 in the RFB compared with FLC-5 monocultures in the RFB and FLC-5 cultured in a monolayer. Mean value ± SD. The ratio of mRNA for each protein versus GAPDH is shown. Differences with respect to each condition were statistically significant ($^bP < 0.01$) according to Student's t-test.

morphology and function. However, three cell lines were studied in our RFB culture system, including their fine structure according to electron microscopy. Layers of FLC-5, A7, and M1 were arranged respectively from the carrier attachment side to the perfusion side. In some areas, liver-like architectures, sinusoid-like lumen structure, bile-canaliculi and functional complex, were observed, comparable to *in vivo* tissue relationship. The M1 cell line well covered the perfusion side, mimicking vascular structures, indicating that this cell type forms an arrangement similar to that *in vivo*. Furthermore, M1 cells in monolayer culture did not express fenestrae, probably reflecting a long culture or subculture time[20]. In a previous study, we found that M1 cells also lack fenestrae in monocultures in the RFB[8]. In contrasts, fenestrated pores were seen in M1 cells cocultured according to the present RFB experimental design. Coculture and cell to cell contact have an influence on these morphological changes. Because fine structures *in vivo* could be observed better than monoculture in the RFB.

The electron microscopic observations in the present study clearly showed that if an appropriate environment for cell growth was provided in a perfusion culture system, the individual cell types could arrange themselves according to their *in vivo* characteristics, even in a high-density layered culture.

This study also examined the numerical dynamics of fenestrae. For this we exposed the cocultures to the actin-disrupting drug swinholide A[14]. When the cells were treated with swinholide A, the number of pores with a diameter of about 100 to 200 nm increased 2 h after swinholide A treatment. Furthermore, by TEM, cytoplasmic vesicles about 200 nm in diameter could be seen and were much larger than the caveolae in the cytoplasm, and their number increased in the presence of swinholide A. These vacuolar-like vesicles probably represent the vesiculo vacuolar organelle (VVO) as described by Feng *et al*[21]. The VVO is an organelle contributing to transport of macromolecules between luminal and abluminal sides of endothelial cells, thus increasing transcellular permeability. Vascular permeability factor and vascular endothelial growth factor (VPF/VEGF) can induce formation of VVO[22]. FLC-5 used in this study, could express VPF/VEGF (data not shown).

The presence of vascular factors may partially explain why VVO is noted in cocultures and why fenestrae could be observed in our experiments[23]. VVO is thought to be formed by fusion of caveolae, when multiple VVOs fuse together, a structure extending from the luminal to the abluminal sides of endothelial cells is formed. In the present study, fused VVOs also were seen in swinholide A - treated specimens by transmission electron microscopy, suggesting that this fusion represents a process culminating in formation of the labyrinthine structures in SEC[24]. The mechanism of pore formation in immortalized SEC and under cocultured perfusion conditions remains unknown from the present study. However, pore formation may result from multiple effects or factors working in concert upon endothelial cells, such as cytoskeletal dynamics represented by actin and/or the influence of a yet unknown factor secreted by other cell types present in the cocultures such as VEGF. The observation that hepatic endothelial cells maintain one of their typical morphological features (i.e. an abundant number of membrane-bound coated-pits, uncoated vesicles/vacuoles and fenestrae) is an indication that the bioreactor mimics a nearby physiological cultivation environment for the various liver cell types. However, the mechanism by which the bioreactor and its culture environment bring about and maintain these membrane-bound vesicles and fenestrae in endothelial cells remain to be elucidated and consequently open up new directions for future experiments.

To assess hepatocyte function, we compared mRNA expression for urea cycle enzymes and albumin synthesis by FLC-5 in monolayer culture compared to these single-type cultures and cocultures in the RFB. Previously, we have demonstrated hepatocyte functions such as albumin synthesis and cytochrome expression are enhanced in the RFB[25, 26]. Urea production is among the most primitive functions of liver cells. We could not detect urea in medium from monolayer cultures or monocultured FLC-5 in the RFB. In contrast, FLC-5 cells cocultured in the RFB exhibit ability to produce urea, and mRNA expression for ASS and ARG is enhanced. The medium used in this experiment, ASF 104 contained arginine, so urea production was observed in cocultures in the RFB although OTC was not expressed. One report showed that urea produc-